Iowa Research Online
The University of Iowa's Institutional Repository

University of Iowa
Iowa Research Online

Theses and Dissertations

2011

# Air entrainment relationship with water discharge of vortex drop structures

Cody N. Pump
*University of Iowa*

Copyright 2011 Cody N. Pump

This dissertation is available at Iowa Research Online: http://ir.uiowa.edu/etd/1062

Recommended Citation
Pump, Cody N.. "Air entrainment relationship with water discharge of vortex drop structures." MS (Master of Science) thesis, University of Iowa, 2011.
http://ir.uiowa.edu/etd/1062.

Follow this and additional works at: http://ir.uiowa.edu/etd

Part of the Civil and Environmental Engineering Commons

# AIR ENTRAINMENT RELATIONSHIP WITH WATER DISCHARGE OF VORTEX DROP STRUCTURES

by

Cody N. Pump

A thesis submitted in partial fulfillment
of the requirements for the Master of
Science degree in Civil and Environmental Engineering
in the Graduate College of
The University of Iowa

May 2011

Thesis Supervisor: Professor A. Jacob Odgaard

Graduate College
The University of Iowa
Iowa City, Iowa

CERTIFICATE OF APPROVAL

MASTER'S THESIS

This is to certify that the Master's thesis of

Cody N. Pump

has been approved by the Examining Committee
for the thesis requirement for the Master of Science
degree in Civil and Environmental Engineering at the May 2011 graduation.

Thesis Committee: _____
A. Jacob Odgaard, Thesis Supervisor

_____
Larry J. Weber

_____
AthanasiosN. Papanicolaou

ACKNOWLEDGMENTS

I would like to thank CH2M HILL and AECOM for allowing me to use data collected from their respective models to analyze for my research.

I would also like to thank Andy Craig and Troy Lyons for helping me with my research and Professor Jacob Odgaard for all of his help with my academics throughout my collegiate career.

Thank you to my parents and family for all of their support and encouragement.

ABSTRACT

Vortex drop shafts are used to transport water or wastewater from over-stressed existing sewer systems to underground tunnels. During the plunge a large amount of air is entrained into the water and released downstream of the drop shaft into the tunnel. This air is unwanted and becomes costly to treat and move back to the surface. Determining the amount of air that will be entrained is a difficult task. A common method is to build a scale model and measure the air discharge and scale it back to prototype. This study investigated a possible relationship between the geometry of the drop structure, the water discharge and the amount of air entrained. The results have shown that air entrainment is still not entirely understood, however we are close to a solution. Using a relationship of the air core diameter, drop shaft length and terminal velocity of the water, a likely exponential relationship has been developed.

TABLE OF CONTENTS

LIST OF FIGURES ..... VI

LIST OF SYMBOLS ..... VII

CHAPTER 1. INTRODUCTION TO VORTEX DROP STRUCTURES .....1

1.1. A brief review of drop shaft literature .....1
1.1.1. Simple air entrainment ratio for a plunging jet .....2
1.1.2. Revised air entrainment ratio for a plunging jet .....3
1.1.3. Analytical and theoretical modeling of air entrainment for a plunging jet .....3
1.1.4. Processes of air entrainment of plunging jets .....5
1.1.5. Volumetric oxygen entrainment of hollow jets .....5
1.1.6. Air entrainment of plunge flow into a pool from a horizontal pipe .....6
1.1.7. CFD modeling of air entrainment of a plunging jet .....6
1.1.8. Theory of air entrainment around plunge .....6
1.1.9. Scaling effects of air entrainment .....7
1.1.10. Drop shaft design criteria .....7
1.1.11. Dimensionless water discharge air entrainment relationship .....7
1.1.12. Air core diameter formula .....8
1.1.13. Tangential inlet velocity .....10
1.1.14. Air entrainment relationship with water jet velocity .....10
1.1.15. Air entrainment of low velocity plunging jets .....10

CHAPTER 2. MODEL DESIGN AND RESEARCH SETUP .....12

2.1. Model Specifications .....12
2.2. Instrumentation .....19

CHAPTER 3. DATA COLLECTION AND METHODOLOGY .....21

3.1. Testing .....21

CHAPTER 4. DATA ANALYSIS AND UNCERTAINTIES .....24

4.1. Air core and length analysis .....24
4.1.1. Analytical air core diameter .....24
4.1.2. Air core ratio formula .....24
4.2. Air core ratio analysis .....26
4.3. Jet velocity analysis .....26
4.4. Dimensionless analysis .....28
4.5. Froude number analysis .....29
4.6. Dimensional analysis .....30
4.7. Uncertainty analysis .....32

CHAPTER 5. AIR ENTRAINMENT RELATIONSHIP .....35

5.1. Best fit relationship .....35

5.2. Scaling Effects .....37
5.3. Example of application .....37

CONCLUSION .....39

REFERENCES .....40

APPENDIX – DATA .....42

LIST OF FIGURES

Figure 1-1: Photo of INDY drop shaft model ..... 2
Figure 1-2: Example of a plunging jet from nozzle into pool of water ..... 3
Figure 1-3: Plan view of tangential inlet ..... 8
Figure 1-4: Profile view of tangential inlet ..... 9
Figure 2-1: WS6 drop shaft layout ..... 13
Figure 2-2: Type H-1 outlet for vortex drop shafts ..... 14
Figure 2-3: AS6 drop shaft layout ..... 15
Figure 2-4: MPS1 drop shaft layout ..... 16
Figure 2-5: ADDS 3D model ..... 17
Figure 2-6: INDY drop shaft layout ..... 18
Figure 2-7: Type H-4 outlet for vortex drop shafts ..... 19
Figure 2-8: Hotwire calibration curve with check ..... 20
Figure 3-1: Spring line depth in the INDY model ..... 23
Figure 4-1: Yu and Lee data vs. results for air core ratio formula ..... 25
Figure 4-2: Air discharge relationship with calculated jet velocity ..... 27
Figure 4-3: Terminal jet velocity vs. air discharge ..... 27
Figure 4-4: Zhao data with current data ..... 28
Figure 4-5: Air concentration vs. Froude number of terminal velocity ..... 30
Figure 4-6: *X* parameter with air core diameter ..... 31
Figure 4-7: Equivalent diameter ..... 31
Figure 4-8: *X* parameter relationship with equivalent diameter ..... 32
Figure 5-1: Best fit relationship ..... 35
Figure 5-2: Standard deviations for best fit relationship ..... 36

LIST OF SYMBOLS

| | |
|---|---|
| A = | Constant |
| $\alpha$ = | Exponent or angle of plunging jet |
| $\gamma$ = | Exponent |
| $\lambda$ = | Air core ratio squared: $d^2/D^2$ |
| $\lambda_C$ = | Coefficient |
| $d$ = | Diameter of air core at throat of vortex |
| $d_e$ = | Equivalent diameter of water cross sectional area |
| $D_j$, $d_j$ = | Diameter of water jet at plunge point |
| $d_n$, $d_0$ = | Diameter of nozzle |
| $D$, $D_s$ = | Diameter of drop shaft |
| $\epsilon$ = | Surface disturbance on jet surface |
| $e$ = | Width of opening from tangential inlet into the drop shaft |
| $Fr$ = | Froude number |
| $Fr_\infty$ = | Froude number of terminal velocity |
| $H_{tot}$ = | Distance from water surface in head tank to plunge point |
| $h_{eqtot}$ = | Head of feeding tank over the vena contracta after orifice |
| $h_j$ = | Height of jet nozzle from plunge point |
| $K_G$, $K$ = | Proportionality coefficient |
| $K_La_{(20)}$ = | Volumetric oxygen transfer coefficient at standard conditions |
| $L$ = | Length of nozzle or height of drop shaft |
| $n$ = | Manning roughness factor |
| $Q$, $Q_w$, $Q_L$ = | Water discharge |
| $Q_a$, $Q_G$ = | Air discharge |
| $\beta$ = | Angle of floor of tangential inlet |
| $\beta_r$ = | Air concentration ratio |
| $r$ = | Radius of water jet |
| $V_X$ = | Horizontal or tangential velocity of water in drop shaft |
| $V_Z$ = | Vertical velocity of water in drop shaft |
| $V_J$ = | Stream wise velocity of water in drop shaft or jet velocity |
| $v_j$ = | Water jet velocity |
| $V_\infty$ = | Terminal velocity of water in drop shaft |
| W = | Circumference of water jet |

# CHAPTER 1. INTRODUCTION TO VORTEX DROP STRUCTURES

Vortex drop structures (or drop shafts) are used to relieve stress on existing drainage systems by creating a secondary drainage system beneath the ground. There are many types of drop structures to transport water or wastewater from the surface to an underground tunnel. Certain scenarios find that using a vortex drop shaft is the most practical solution. Unfortunately, unwanted air is entrained into the water when the vortex plunges into the pool. The air then is released downstream of the drop shaft into a de-aeration chamber or tunnel. The air then needs to be returned to the surface or treated at the end of the tunnel. Treatment can be expensive in both capital and operating costs. Design optimization for the drop structures that lead into a chamber or tunnel is necessary to minimize costs in all aspects. This includes designing a treatment center with the capacity to process all incoming air or designing a return shaft for to the surface. The amount of air that will be entrained is difficult to estimate. There is currently no method to predict the quantity of air for a given drop structure, other than building a scale model and measuring it. The theory of this research is to determine a relationship between the water discharge, the dimensions of the structure, and the air that will be entrained.

## 1.1. A brief review of drop shaft literature

In the following section, a review of previous drop shaft, plunge flow and air entrainment studies will be discussed. Most of the articles reviewed focused on jets plunging into a pool of water through the atmosphere or plunge drop shaft flow. As they are related hydraulically, they are discussed to exam the physical properties of air entrainment. Through understanding the physics and variables responsible for determining the amount of air that will be entrained in many scenarios, will come the solution to this study.

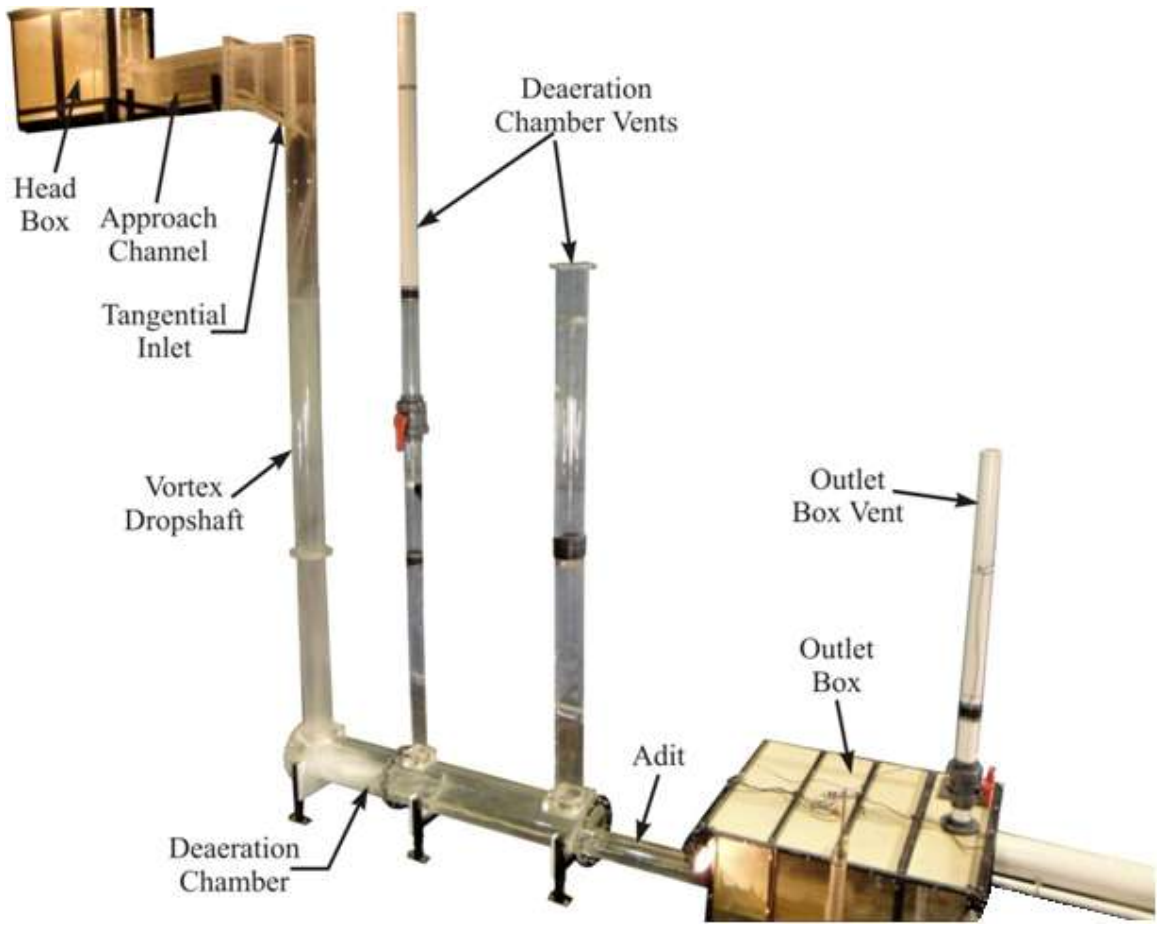


Figure 1-1: Photo of INDY drop shaft model

### 1.1.1. Simple air entrainment ratio for a plunging jet

Bagatur and Sekerdag (2003) studied the effect of the shape of the jet on the air entrainment relationship. They used a rectangular jet with rounded edges and measured the air entrained for a jet plunging into a pool at 45 degrees. They compared their results with Henderson et al. (1970) who stated that the entrainment ratio for circular jets is defined by:

$$\frac{Q_a}{Q_w} = \left(\frac{d_j}{d_n}\right)^2 - 1 \qquad (1\text{-}1)$$

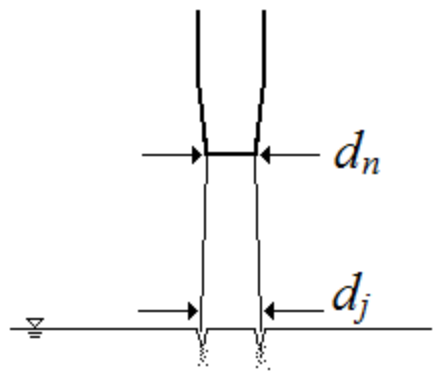


Figure 1-2: Example of a plunging jet from nozzle into pool of water

Bagatur and Sekerdag found that the ratio worked for the rectangular jets as well, showing that air entrained by the jet was independent of the shape. This is a theory that will be applied to the vortex drop shaft in the analysis of this study.

### 1.1.2. Revised air entrainment ratio for a plunging jet

McKeogh and Ervine (1980) studied the factors that govern the air entrainment rate of plunging jets. Similar to Bagatur and Sekerdag (2003), they compared their results to Henderson et al. (1970). Through their study, they found that the ratio was related to the surface roughness of the jet ($\epsilon/r$), rather than just the diameter. The relationship derived from their results states:

$$\frac{Q_a}{Q_w} = 1.4\left[\left(\frac{\epsilon}{r}\right)^2 + 2\left(\frac{\epsilon}{r}\right) - 0.1\right]^{0.6} \tag{1-2}$$

### 1.1.3. Analytical and theoretical modeling of air entrainment for a plunging jet

Gualtieri and Doria (2006) focused on theoretical modeling of air entrainment by using a previous equation developed by Gualtieri and Doria (2000), where $\beta_r$ is the air

concentration, $K_G$ is a proportionality coefficient, $H_{tot}$ is the total distance from between the water surfaces and $h_{eqtot}$ is the head over the vena contracta, which stated:

$$\beta_r = K_G \left(\frac{H_{tot}}{D_s}\right)\left(\frac{h_{eqtot}}{D_s}\right) \tag{1-3}$$

In the new study, this equation was transformed using more variable that include foamy height of water around the jet known as the air tore height. The final model developed through various modeling and reduction was:

$$\beta_r = K \left(\frac{H_{tot}}{D_s}\right)^{\alpha} \left(\frac{h_{eqtot}}{D_s}\right)^{\gamma} \tag{1-4}$$

This provided a better fit for their data and allowed for an air entrainment prediction law for plunging jets based on several values of $h_{eqtot}/D_s$ when using the values of $K$=0.00425, $\alpha$=0.81 and $\gamma$=0.83.

Luca, Paolo and Guelfo (2008) used Gualtieri and Doria (2006) as a base equation to manipulate into a better fit for their model. Using further analysis of the model's dimensionless variables, and integration of experimental data to develop a Gaussian curve for the constant 'K', they concluded that the following expression represents the air entrainment ratio:

$$\beta_r = Aexp\left\{-\frac{[ln((d/D-0.25)/(1.28-d/D))]^2}{\lambda_c^2}\right\}\left(\frac{H_{tot}}{D}\right)^{\alpha}\left(\frac{h_{eq}}{D}\right)^{\gamma} \tag{1-5}$$

The constants in the expression are determined through application of experimental data once again. The values determined to provide the best fit were: A= $5.446*10^{-3}$; $\lambda_c^2$ = 2.067; d/D ranges from 0.25 to 1.28; α = 0.918 and γ = 0.823. The $\lambda_c$ here is a coefficient and not the air core diameter ratio.

### 1.1.4. Processes of air entrainment of plunging jets

Chanson and Manasseh (2003) studied the physical properties of air that is entrained from a plunging jet. It was found that there are three regimes of air entrainment. These regimes are related physically to the velocity of the jet and the height of air through which it falls. Regime I (when jet velocity reaches the minimum magnitude for air entrainment) has very fine bubbles entrained at a relatively slow rate. In regime II (when the air cavity around the perimeter of the jet at the plunge point becomes unstable), which occurs at a jet velocity of 1 m/s, the air entrained increases notably. For the highest velocity jet (a velocity of 3.5 m/s or higher) in regime III (when the air cavity along the perimeter of the jet at the plunge point is elongated and broken up into the plunge pool), a spike was found in the number of 1 mm air bubbles entrained.

### 1.1.5. Volumetric oxygen entrainment of hollow jets

Deswal (2009) used the theory of oxygen transfer to determine the entrainment rate. Using an equation from Sande and Smith (1975), the formula was used to derive a relationship from the experimental data collected. The relationship found that the transfer rate was directly linked to the velocity of the jet. The formula was then manipulated using a multivariate linear regression to develop the following relationship between the oxygen transfer rate ($K_L a_{(20)}$) and the jet velocity parameters where $n$ is the Manning's roughness factor, $v_j$ is the jet velocity and $d_j$ is the diameter of the jet at the plunge point:

$$K_L a_{(20)} = 0.103 n^{0.81} v_j^{2.11} d_j^{1.43} \tag{1-6}$$

### 1.1.6. Air entrainment of plunge flow into a pool from a horizontal pipe

Smit (2007) based his thesis on the study of air plunging into a pool of water from a horizontal pipe. The study focuses on the penetration depth of the plunge and the air entrainment related to the depth. The results show an increase of air entrained with increasing water discharge and fall height. No relationship was defined from the results; however the review of air entrainment literature was thorough and led this study towards a more refined relationship.

### 1.1.7. CFD modeling of air entrainment of a plunging jet

Schmidtke and Lucas (2008) used CFD modeling of an impinging jet into a pool of water to verify the theory of Ohkawa et al (1986), where $Q_G$ is the air discharge, $Q_L$ is the water discharge, $h_j$ is the height from the jet nozzle to the water and $d_o$ is the diameter of the nozzle, which states:

$$\frac{Q_G}{Q_L} = 0.016\left[Fr^{0.28}\left(\frac{h_j}{d_0}\right)^{0.4}\right]^{1.17} \qquad 1\text{-}7$$

This relationship states that the entrainment of air is related to the Froude number of the jet. This was not accurate enough for the CFD model to work correctly so a coefficient of drag function of the bubbles entrained was introduced.

### 1.1.8. Theory of air entrainment around plunge

Chanson and Brattburg (1998) studied the effects of a jet impinging into a pool of water to develop a formula for the flow region of the very-near field (a depth within 5 times the diameter of the jet). The results showed that the understanding of air entrainment is not well understood. However, the water surface near the jet forms an induction trumpet in which the water is pulled under the surface with the jet. The

velocity of the water near the jet was found to be a function of the jet velocity and velocity at which air entrainment begins.

### 1.1.9. Scaling effects of air entrainment

Chanson (2008) analyzed the scaling effects of various air-water interfaces. Jet plunge flow was determined to be similar to a horizontal hydraulic jump with a different diffusion pattern. The effects of scaling were determined to be: the fluid properties (density, viscosity, surface tension etc.); geometry of the structure; and the plunge properties (inflow depth, velocity, turbulent velocity, and boundary layer thickness). Using dimensionless analysis, among the numerous ratios created for scaling, the well-known Froude, Reynolds and Weber numbers are found and the relationship may be expressed using only the properties of water.

### 1.1.10. Drop shaft design criteria

Jain (2004) investigated the hydraulic performance of different types of drop structures. The main two drop shafts were plunge-flow and vortex-flow structures. The vortex-flow structure was determined to have "superior hydraulic performance" when considering air venting and other various criteria. A derivation of the Manning equation is given that determines the terminal velocity ($V_\infty$) of water falling as an annular jet:

$$V_\infty = \left(\frac{1}{n}\right)^{3/5} \left(\frac{Q}{\pi D_1}\right)^{2/5} \tag{1-8}$$

### 1.1.11. Dimensionless water discharge air entrainment relationship

Rajaratnam (1997) mainly focused on the hydraulics of drop shafts and while measuring the air entrained, simply plotted the entrained air concentration against the dimensionless water discharge. This shows a trend that could be developed into a

relationship between the two upon further experimentation. The dimensionless water discharge is essentially a Froude number.

### 1.1.12. Air core diameter formula

Jain and Kennedy (1983) researched extensively the hydraulics of many drop shafts including vortex drop shafts. After determining that vortex drop shafts are hydraulically superior to other types, experiments were done in which the air core diameter at the throat of the core was measured. From this a formula was developed to predict the diameter of the core given the water discharge and properties of the structure:

$$\sqrt{\frac{(1-\lambda)^3}{2\lambda}} = 4\left(\frac{Q^2 e}{g\pi^3 D_1^6 \cos^4\beta}\right)^{1/3} \tag{1-9}$$

$\lambda$ is the air core diameter ratio: $d^2/D^2$, $e$ is the width of the opening into the drop shaft from the tangential inlet, shown in Figure 1-3, and $\beta$ is the angle of the floor of the tangential inlet, shown in Figure 1-4. The angle of the horizontal approach to the tangent is θ, but it is not used for this study.

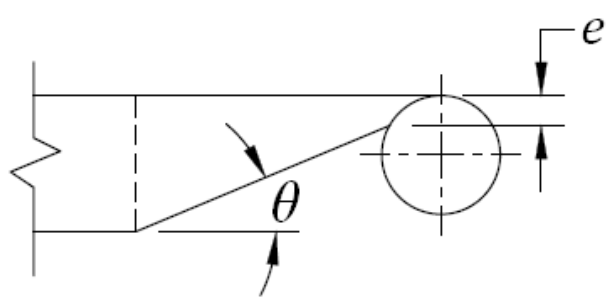


Figure 1-3: Plan view of tangential inlet

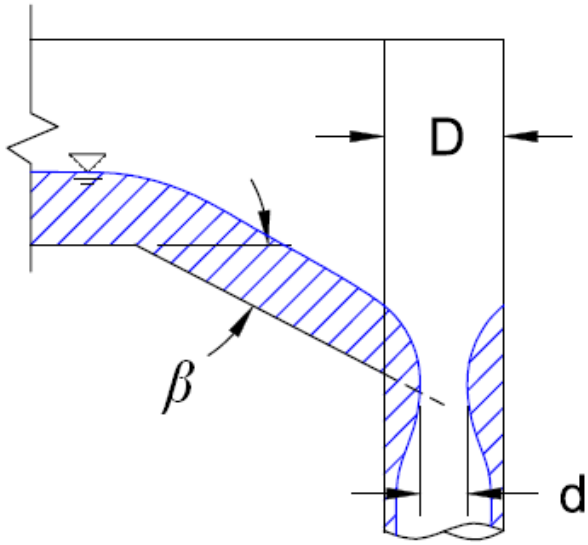


Figure 1-4: Profile view of tangential inlet

Yu and Lee (2009) revised the design criteria for vortex drop shafts. While studying the hydraulics of the inlet geometry, the air core theory was derived using a tangential velocity from a free vortex rather than a constant to obtain:

$$\sqrt{\frac{(1-\lambda)^3}{2\lambda^2}} = 4\left(\frac{Q^2 e}{g\pi^3 D_1^6 \cos^4\beta}\right)^{1/3}\left(\frac{1}{(1-e/D)}\right) \tag{1-10}$$

This theory was plotted against Jain and Kennedy (1983) data and measured data to show that the air core theoretical equations both are still not entirely accurate at predicting the actual measured diameter. While the data does tend to follow the trend of the prediction, the error could be as much as 20% different from predicted to measured, for the upper range of the air core ratio. The right hand side of this equation will be referred to as “RHS” here after.

### 1.1.13. Tangential inlet velocity

Jain (1984) analyzed the hydraulic performance of tangential vortex inlets and developed two equations for the velocity of the flow inside the drop shaft at the throat of the air core. The horizontal velocity component is given by:

$$V_x = \left(\frac{gQ}{e}\right)^{1/3} (\cos\beta)^{4/3} \tag{1-11}$$

The vertical velocity component is given by:

$$V_z = V_x \left[\frac{1-\lambda}{2\lambda}\right]^{0.5} \tag{1-12}$$

### 1.1.14. Air entrainment relationship with water jet velocity

Zhao, Zhu, Sun and Liu (2006) studied the performance of vortex drop shafts and determined that the air entrained relates to the velocity of the jet just before the plunge. A correlation was given using the width of the water jet and a coefficient to obtain:

$$Q_a = \lambda_c W \left[0.00002\left(V_j - 1\right)^3 + 0.0003\left(V_j - 1\right)^2 + 0.0074\left(V_j - 1\right) - 0.0058\right] \tag{1-13}$$

Zhao also proposed an equation for the vertical velocity of the water from continuity with the thickness of the water (t) against the wall of the drop shaft is:

$$V_z = \frac{4Q}{\pi D^2 t(2-t)} \tag{1-14}$$

### 1.1.15. Air entrainment of low velocity plunging jets

Sande and Smith (1976) researched a way to relate the air entrainment of a jet by combining several variables into what will later be called the ‘X’ parameter. Deriving a

base equation from kinetic energy analysis and the angle of attack, the following equation was found to fit the data quite well once the exponents were solved for:

$$Q_a = 0.015\left(\frac{D_j^2 V_j^3 L^{1/2}}{\sin^{1.5}\alpha}\right)^{3/4} \tag{1-15}$$

This equation was for plunging low velocity jets with long cylindrical nozzles where $D_j$ is the diameter of the jet and $L$ is the length of the nozzle. The $X$ parameter is the combination of variables inside of the parentheses.

Bin (1993) used Sande and Smith (1976) to establish that the equation worked for other applications. Bin defined the $X$ parameter as:

$$X = D_j^2 V_j^3 L^{1/2} \sin^{-1.5}\alpha \tag{1-16}$$

From there, the data from a low velocity jet with a short cylindrical nozzle was fit to the air entrainment to develop the following relationship:

$$Q_a = 0.0076X^{0.75} \tag{1-17}$$

This relationship has the same slope and is within the same ranges as the Sande and Smith (1976) data. This theory used the diameter, velocity and length of the jet as the main variables for air entrainment. This study showed that the $X$ parameter can be used for different applications and still fit experimental data very well.

# CHAPTER 2. MODEL DESIGN AND RESEARCH SETUP

For this study, two scale models were used for the collection of data. The first model is a multi-drop shaft design with three separate vortex drop shafts that have unique designs. Each drop shaft has a 4” vent pipe attached to the approach channel with a hot wire transducer installed. Each drop shaft discharges into a main tunnel system that leads to a tail-box, which is used to set the water level in the tunnel. The system is air-tight except for the inlet vents and outlet vent at the end of the tunnel. The outlet vent is also monitored with a hot wire. For the purpose of this research, the tunnel was open to atmospheric conditions to prevent any pressure in the tunnel.

The second model used is a single vortex drop shaft that has a longer drop than all three drop shafts in the first model. The model is setup so that the inlet leading to the vortex generator is open to atmospheric conditions without constraints. The drop shaft plunges into a de-aeration chamber that has a 4” vent pipe that has a hot wire installed. The de-aeration chamber leads into an adit pipe that discharges the water into a tail-box. The tail-box can set the water level in the model and also has a monitored 4” vent pipe.

## 2.1. Model Specifications

The first model, labeled “ADDS” has three drop shafts labeled “AS6”, “WS6” and “MPS1”. Each drop shaft has a different inlet or outlet so as no two are alike. The WS6 drop shaft has a tangential type vortex generator with a new type of design for the outlet. The outlet design for WS6 allows for the drop shaft to plunge the vortex into the top of a box about one-third of the distance from the back of the box. The front of the box discharges the water into a tunnel just below the centerline at a right angle to the flow in the tunnel. The front of the box has baffle walls along both sides so as the water creates a back-up of water inside the box. The sharp corners dissipate energy efficiently while the pooled water decreases potential erosion due to cavitation. The WS6 drop shaft model design specifications are shown in Figure 2-1.

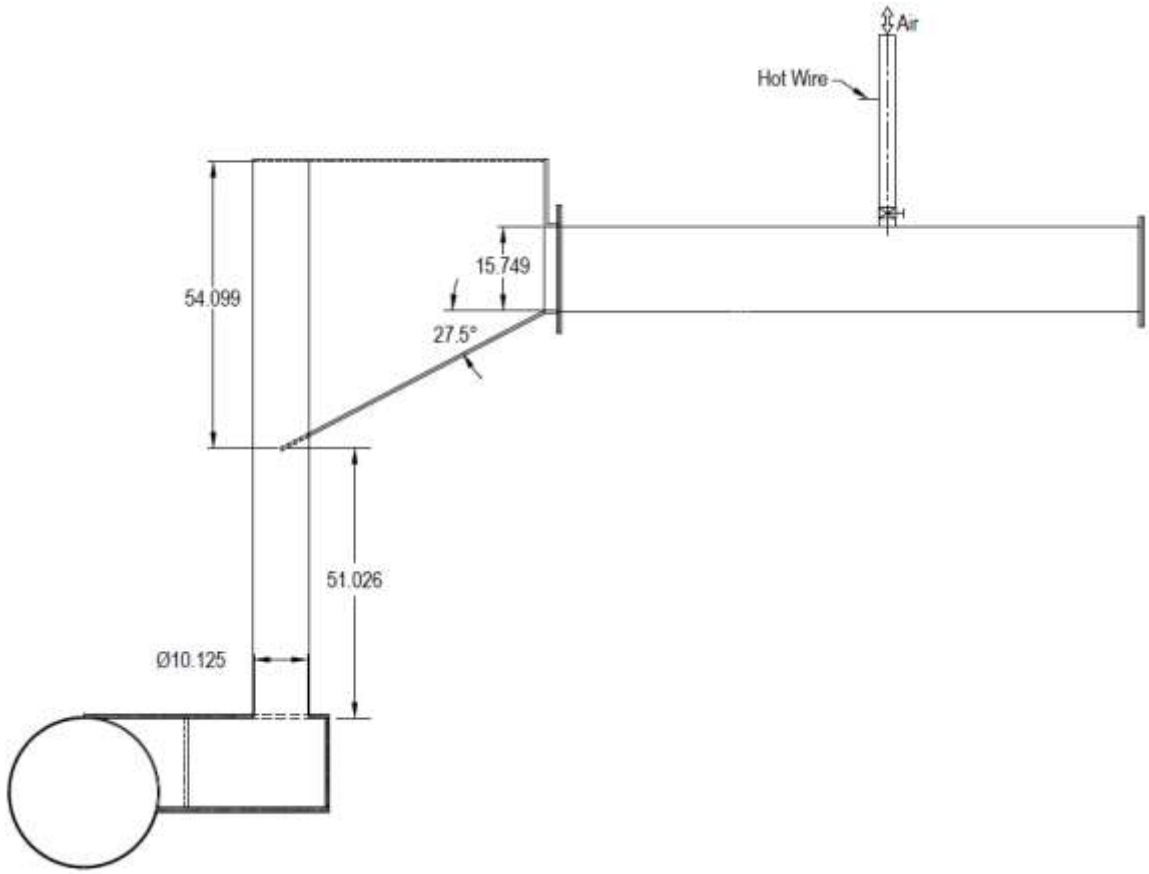


Figure 2-1: WS6 drop shaft layout

The AS6 drop shaft has an H-1 type outlet that vents into the main tunnel with a unique inlet design. Rather than the typical tangential inlet that requires one wall to intersect the drop shaft at a tangent while the opposing wall angles into the opening, the AS6 inlet has a widening of the approach channel into a preliminary inlet box structure where both walls angle towards the drop shaft tangential inlet. This design was implemented to eliminate any hydraulic jump in the tangential inlet. The design specifications are shown in Figure 2-3. The outlet directs the water through a manhole structure then into a down-step ramp into the tunnel.

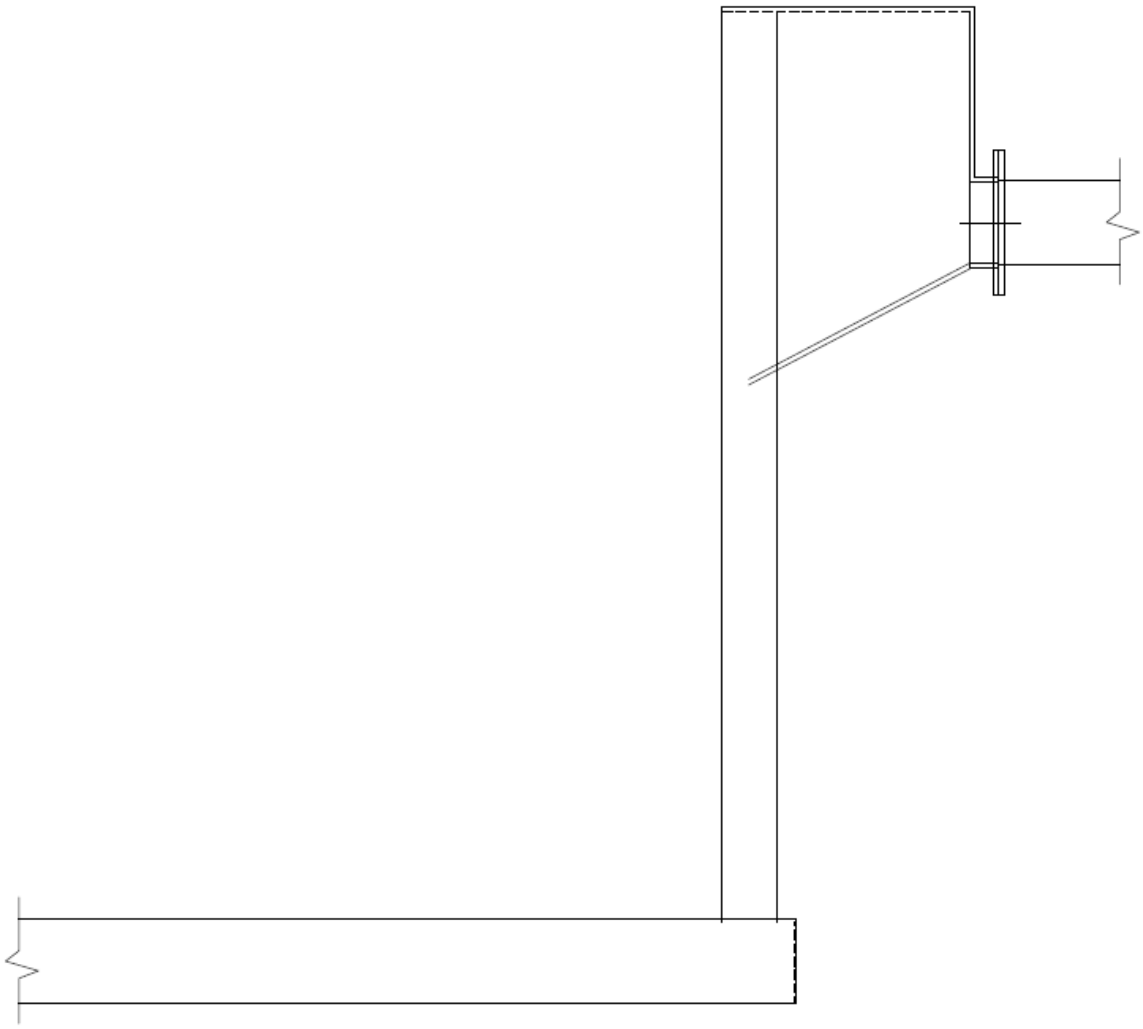

Figure 2-2: Type H-1 outlet for vortex drop shafts

An H-1 type outlet typically has a secondary tunnel perpendicular to the drop shaft that feeds the water into the main tunnel. This tunnel is usually a constant diameter for the entire length. The H-1 can have a vent for air that goes either back to the surface or to the top of the tangential inlet to recycle the air. In the case of AS6 and MPS1 drop shafts, the vent is not included so that the air is directed into the main tunnel for the purpose of a controlled air flow direction when in operation. Jain and Kennedy (1983) have a comparison of all 6 types of outlet configurations.

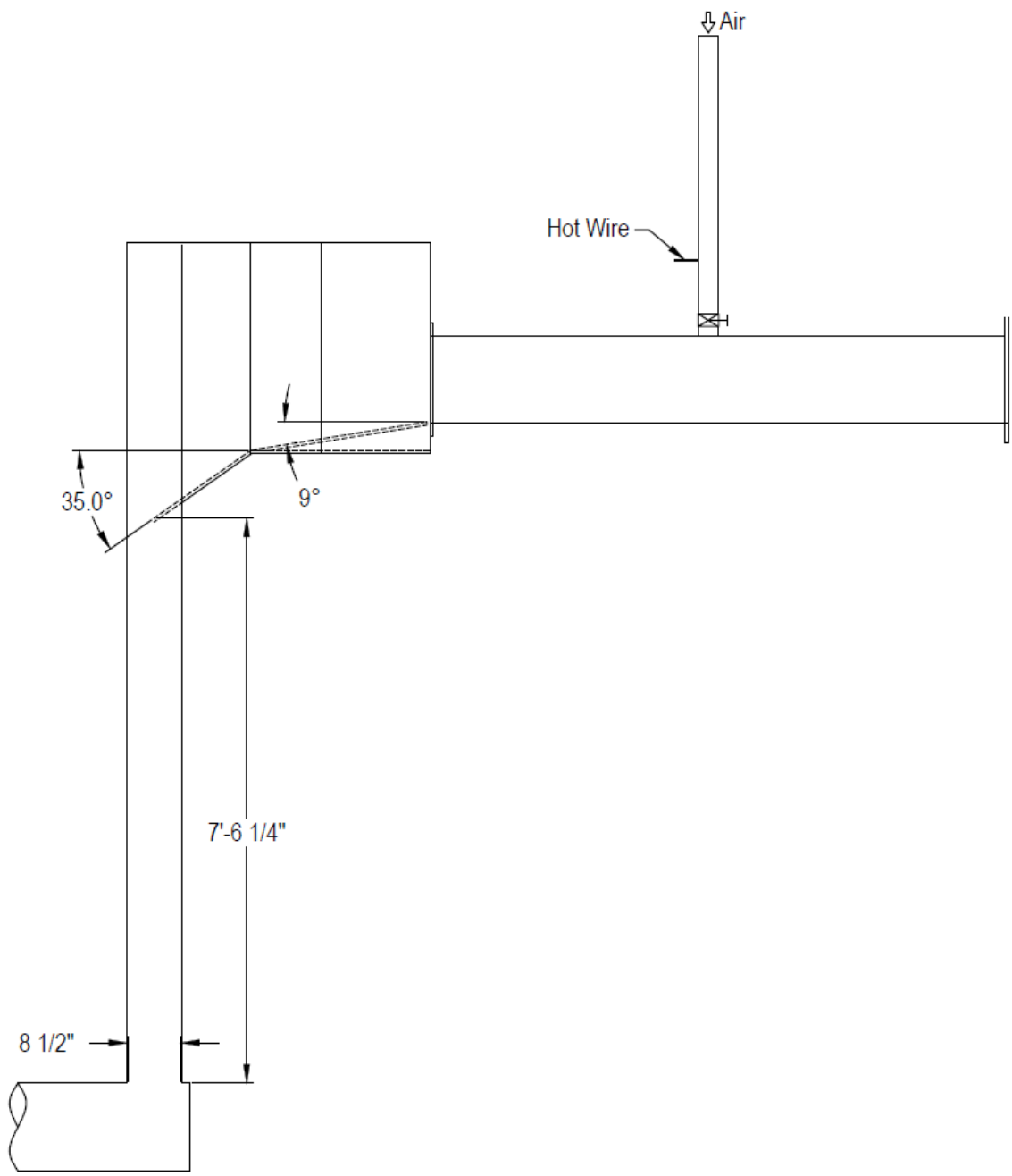


Figure 2-3: AS6 drop shaft layout

MPS1 drop shaft has a tangential inlet similar to the WS6 drop shaft and an H-1 type outlet. This drop shaft is scaled down smaller than both AS6 and WS6. The outlet leads into the main tunnel via a long adit conduit and enters the tunnel down a stair-step energy dissipater. The specifications are given in Figure 2-4. A perspective view of the entire ADDS model is shown in Figure 2-5.

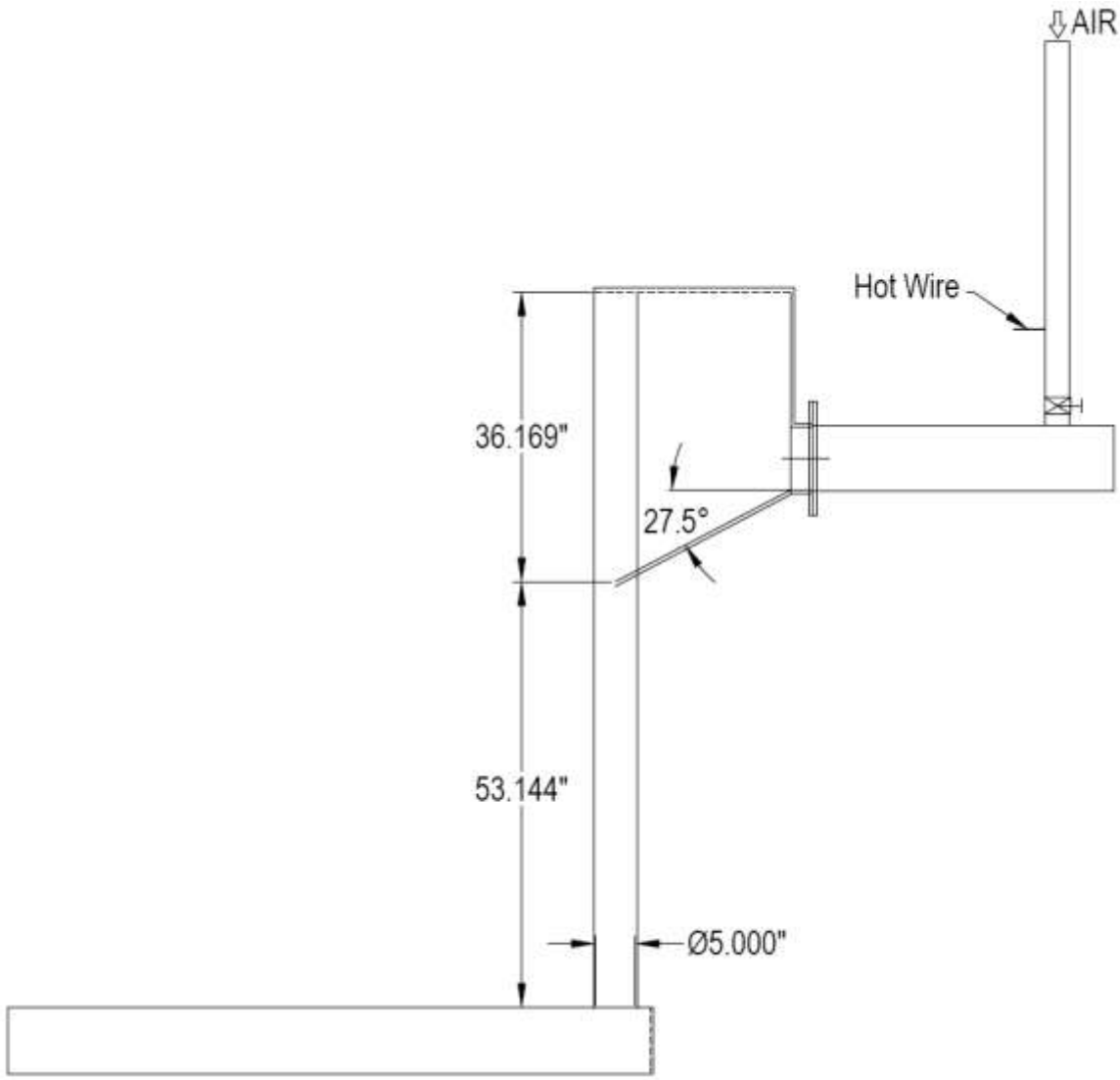


Figure 2-4: MPS1 drop shaft layout

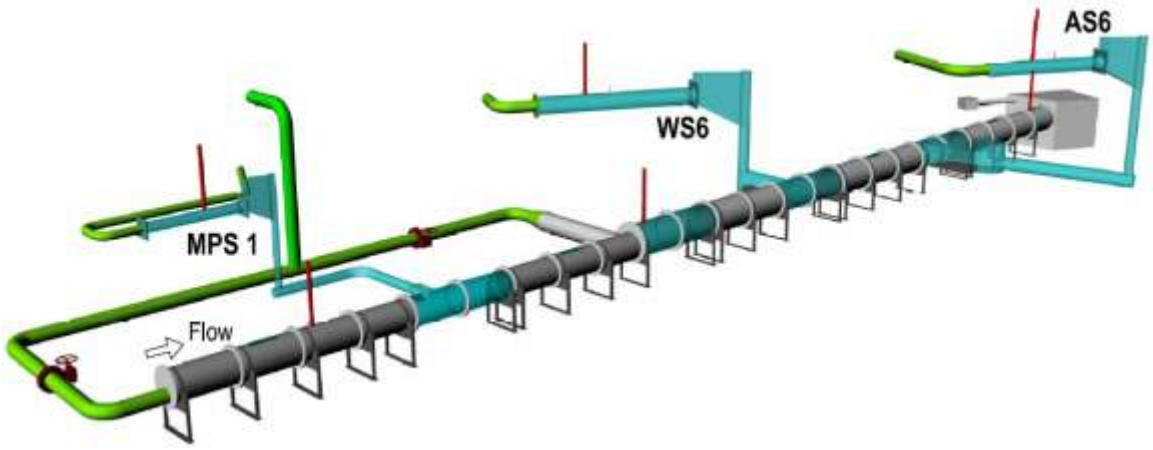


Figure 2-5: ADDS 3D model

The second model labeled "INDY" has one drop shaft with a simple tangential inlet with an H-4 type outlet that includes a de-aeration chamber with an air vent that connects to a main tunnel through an adit. The model simulates the main tunnel using the tail box with a valve-controlled outlet. The INDY model specifications are shown in Figure 2-6.

A typical H-4 type outlet, shown in Figure 2-7, has a large secondary tunnel that suddenly contracts into a smaller diameter tunnel that then feeds the water into the main tunnel. The larger tunnel that the drop shaft plunges into is called the de-aeration chamber. The chamber has a vent for the entrained air to escape back to the surface or be recycled back into the tangential inlet. The purpose of an H-4 type outlet is to capture all of the air before the water discharges into the main tunnel. The contraction of the tunnel serves as an orifice and is usually designed to create a backup of water that submerges the smaller tunnel, forcing all of the air out of the de-aeration chamber vent.

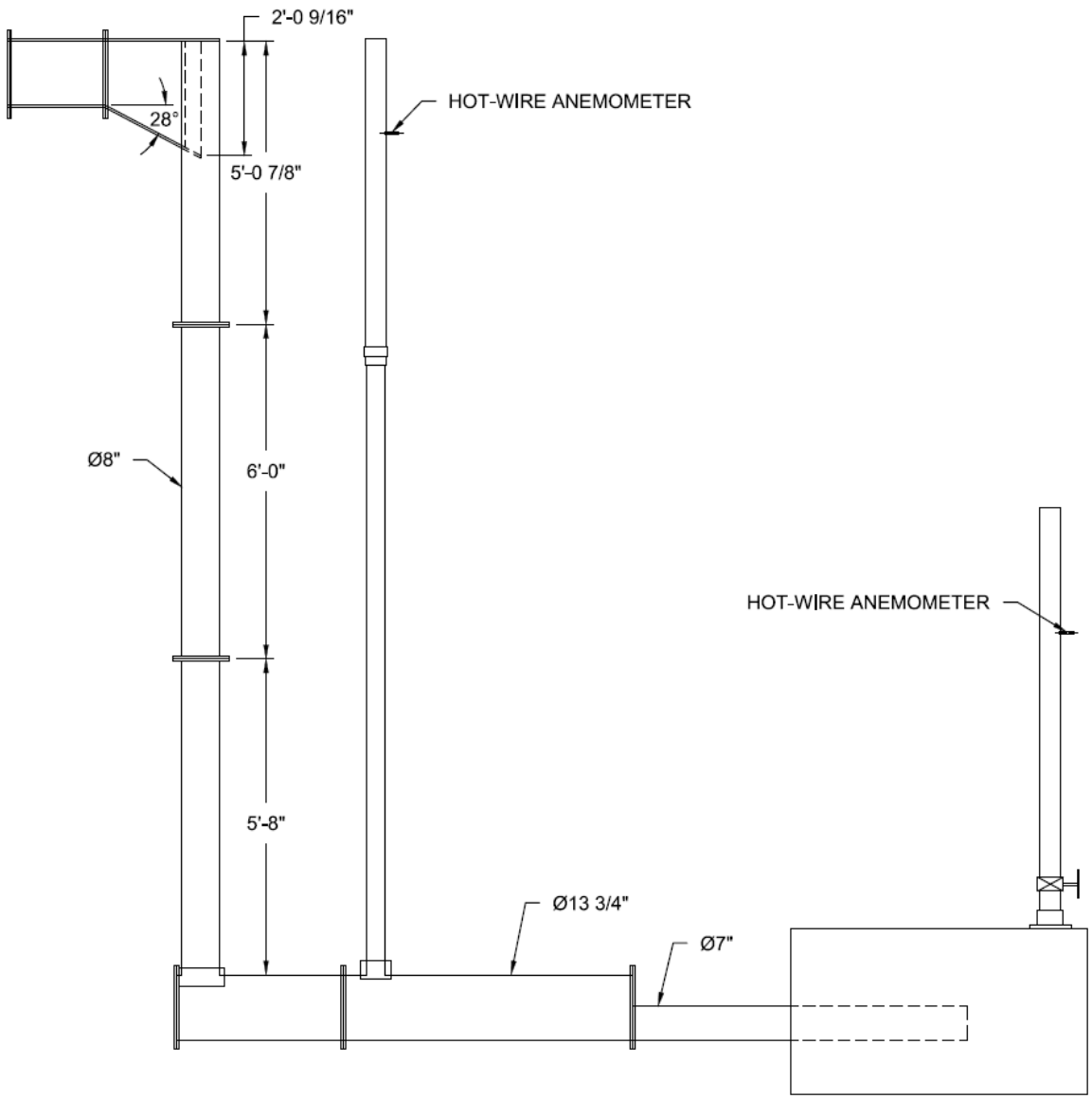


Figure 2-6: INDY drop shaft layout

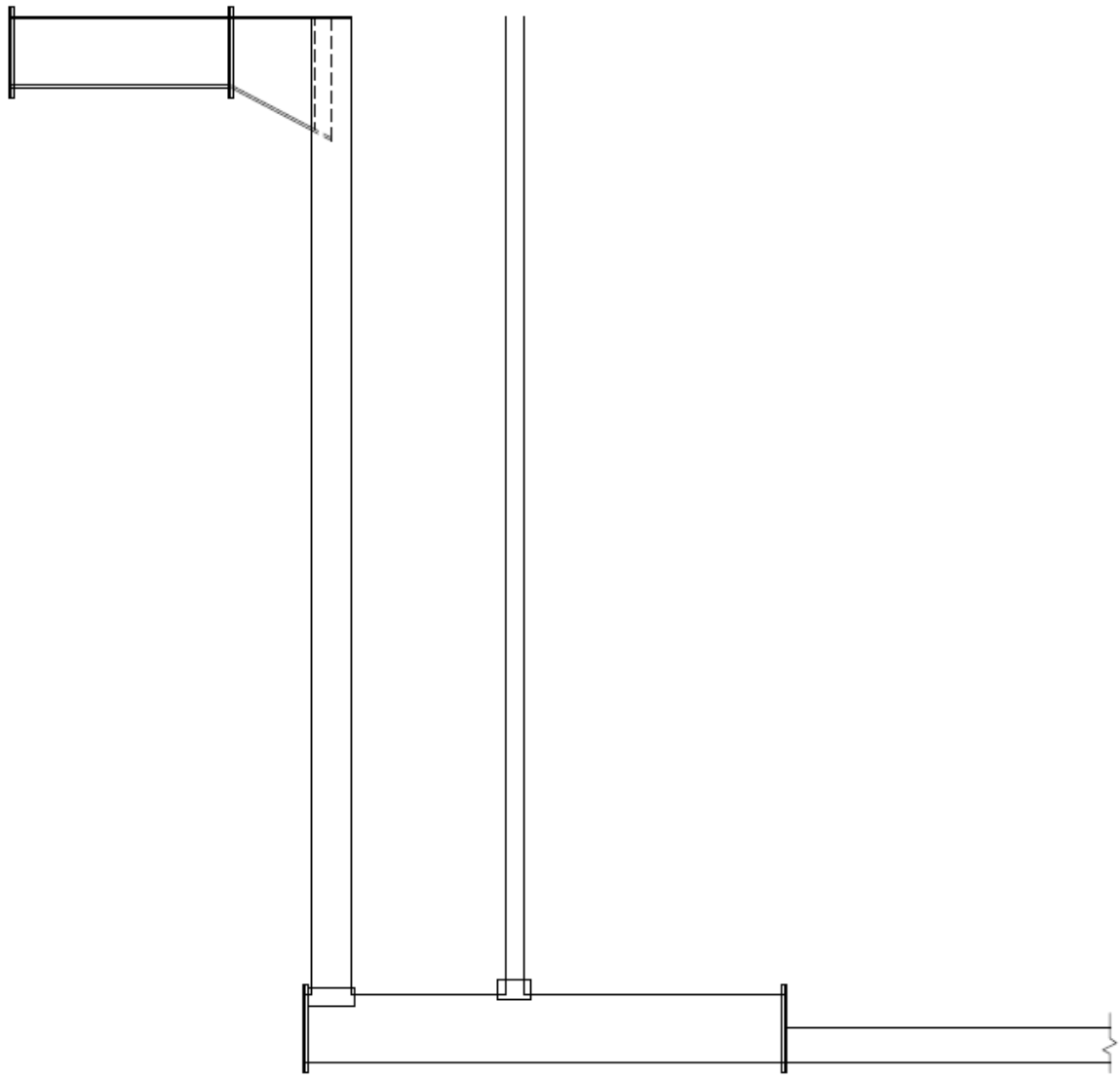

Figure 2-7: Type H-4 outlet for vortex drop shafts

## 2.2. Instrumentation

The hot wire transducers used for all models were TSI Air Velocity Transducer Model 8455 hotwire anemometers. The hotwire anemometers were calibrated in-situ by IIHR. The hotwires were installed in the vent pipes with the ceramic heating element of the hotwire positioned in the center of the pipe. The airflow through each standpipe was controlled using an extraction fan at a constant speed. Upon reaching steady state, an

Alnor Model RVA801 vane anemometer was mounted to the vent pipe and the average air velocity was measured over a period of 30 seconds. The average voltage output from the hotwire was recorded simultaneously. The airflow was established at steady state for several fan speed settings in order to bracket the expected range of air flows during model tests. A linear calibration curve resulted for each hotwire. A representative curve, as shown in Figure 2-8, converted voltage into velocity (m/s).The calibrations were checked periodically to ensure repeated accuracy. The accuracy of the hot wire anemometer is specified to be +/- 2% of the reading.

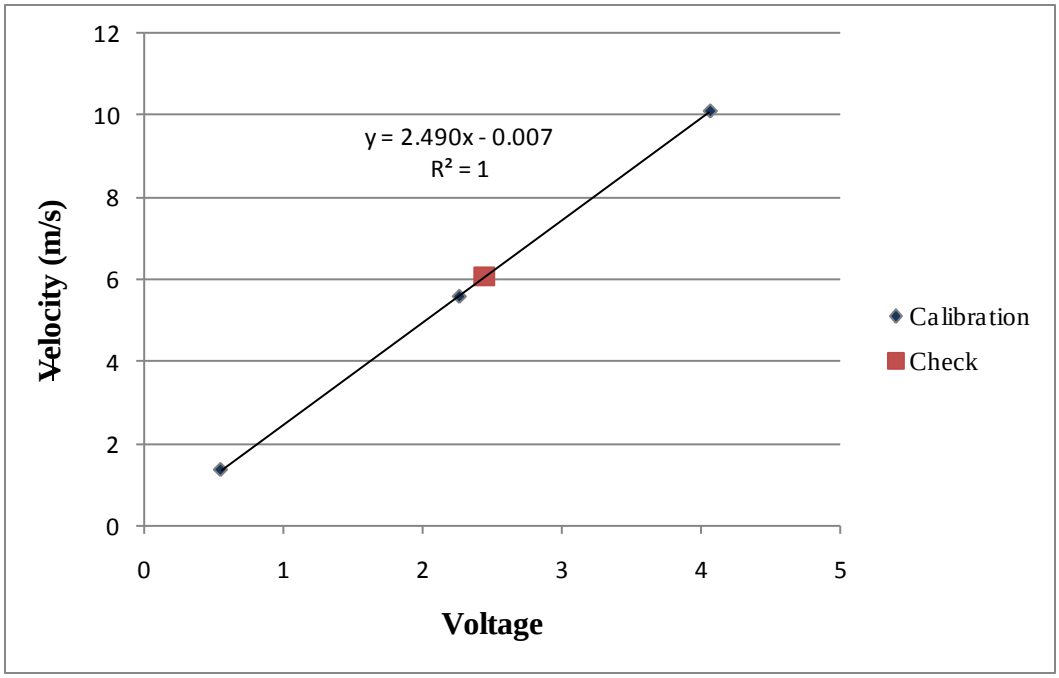


Figure 2-8: Hotwire calibration curve with check

The direction of air flow was determined with the Alnor rotating vane anemometer. The manufacturer specifies accuracies of +/- 1% of the reading between 50 to 6,000 ft/min. The vane anemometer features a 4-inch diameter bore allowing direct adaption to the 4-inch air outlet vents on the model.

# CHAPTER 3. DATA COLLECTION AND METHODOLOGY

The data was collected using a software program called LabVIEW. All hot wires were connected to a computer through an automated data-acquisition system. The display showed live data output allowing steady-state to be seen visually before any data was acquired. LabVIEW records the data into tabulated text files for each test run. The frequency can be set manually in the user interface, which was set to 100 Hz. The typical test was recorded for 60 seconds. This gives a total of 6000 data points that can be averaged.

For the ADDS model, each drop shaft was run independently. The stand pipes for all drop shafts were closed except the one in use and the tunnel outlets. This kept the tunnel from building up any pressure that would alter the air discharge from the drop shafts. For the INDY model the air was measured downstream of the drop shaft in the de-aeration chamber and in the tail box. The values used were the summation of the two air vents for a total air discharged.

For each test a water discharge was set as a percentage of the design flow. To determine the flow rate, a manometer was used in junction with an orifice plate that has a predetermined coefficient. The orifice plate was installed upstream of the valve for each drop shaft. Each orifice plate has its own size and coefficient. The AS6 drop shaft used an elbow meter installed upstream of the valve in junction with the manometer. The MPS1 drop shaft used both an elbow meter and orifice plate upstream of the valve to ensure a broad enough range of flows could be accurately measured to an acceptable number of significant digits.

## 3.1. Testing

The ADDS model tests were run to include data from a wide range of flow rates. Each drop shaft was tested at 14 flow rates as a percentage of the design discharge. The percentage of design discharge ranged from 10% to 140% in 10% increments. For the

MPS1 drop shaft, a repeated test was performed for 40%, 100% and 140% flows. For the AS6 and WS6 drop shafts, a repeated test was performed for all even percentages (i.e. 20%, 40%, 60%, etc.). The INDY model was run at flow rates of 10%, 25%, 50%, 75% and 100% of the design discharge. The model had a limiting peak discharge of 117% due to geometric constraints of the approach channel. Consequently, no data was collected above the design discharge. The 5 flow rates tested on the INDY model were repeated numerous times using several different methods to measure the air discharge. Using calibration and instrument error probabilities, the most accurate instrument for measuring the air discharge was the hot wire anemometers. The final test series was performed and used for this study.

The tunnel water depth for the ADDS model tests was self-setting based on the discharge of the drop shaft. The tunnel discharges into a tail box that is outlet controlled. The tunnel is elevated above the floor of the box and the outlet is located in a sub-floor chamber. The water is required to pass through a perforated plate in the floor to enter the chamber. This allows the valve of the outlet to be closed enough to back up the water until the depth is above the perforate plate and below the tunnel invert. The water depth assures that any air that may be entrained into the tail box water will be able to rise out of solution before exiting the model. The outlet is kept fully submerged for all tests to eliminate any possibility of air leaving through the un-monitored outlet.

The water depth in the INDY model was kept at a depth known as “spring line depth.” The spring line depth is a percentage of the adit tunnel height that was determined to be the depth at which the main tunnel would back up water into the drop structure in the field. In model units, the spring line depth is 4.67 inches of the 7 inch adit inner diameter, or 67 percent. The spring line depth can be seen in Figure 3-1. This pre-determined depth had minimal effect on the air discharge for the 2 tests in which the adit tunnel had a free surface of water from the de-aeration chamber. For the higher water flow rates, the adit remained submerged at the entrance from the de-aeration

chamber. This assured that no air was freely entering the tail box. Air measurements of the tail box confirmed this assumption.

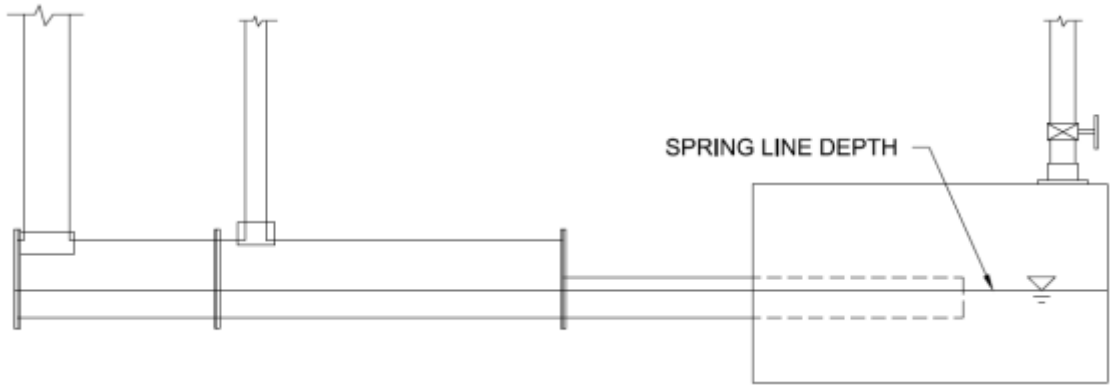


Figure 3-1: Spring line depth in the INDY model

For all tests in the INDY model, the water leaving the tail box must also pass through a perforated plate close to the floor of the box. The short height of the perforated plate allowed the depth of the water in the tail box to be relatively low and still maintain a submerged outlet. The plate was attached to a sealed chamber that disconnected any air or water from entering other than the designed opening. The spring line depth was significantly higher than the minimum depth required for a submerged outlet. The depth in the tail box was measured using a point gage attached to the outside of the box in a stilling basin that had a feed line into a low-turbulence region. The point gage setup allowed for very steady measurements due to a large buffer that eliminated any waves or spikes in water depth inside the tail box.

# CHAPTER 4. DATA ANALYSIS AND UNCERTAINTIES

All of the data was imported into Microsoft Excel and combined into large tables of raw data. The data was then paired with geometric specifications for each drop structure. Using theories from the literature review, many hypothesis were developed in attempt to find the relationship between the air entrainment, water discharge and drop shaft geometry.

## 4.1. Air core and length analysis

### 4.1.1. Analytical air core diameter

Using the geometry, the predicted diameter of the air core for each water discharge was calculated. The air core diameter for each test was determined using Equation 1-9 from Jain and Kennedy (1983). The air core was then calculated with the Yu and Lee (2009) revised formula, Equation 1-10. The two were compared and showed similar results with difference ranging from 0 to 15%. The majority of the diameter differences were less than 6%. The greatest error came from higher flows in the WS6 drop shaft, which was also considered hydraulically unstable at those same flows where a hydraulic jump occurred in the inlet.

### 4.1.2. Air core ratio formula

The air core diameter was measured indirectly for a select few flow rates of all three ADDS drop shafts and all flow rates of the INDY drop shaft. The values were compared with the Yu and Lee data and Equation 1-10. A linear relationship, shown in Figure 4-1, appears when plotting Yu and Lee's data against the analytical formula they developed. The linear relationship values from Equation 4-1 were used for the remaining calculations since the Yu and Lee geometry and water discharge was used to calculate the RHS of their formula and given that the current data fell into the same prediction of the Equation 1-10, it can be assumed that the current data will fall along the Yu and Lee

measured data. The air core diameters for the current data could not be measured directly due to the model designs. Equation 4-1 could also be seen as an easier method to solve for the air core ratio using the RHS of Equation 1-10, given by:

$$\lambda = -0.6 \cdot RHS + 0.96 \tag{4-1}$$

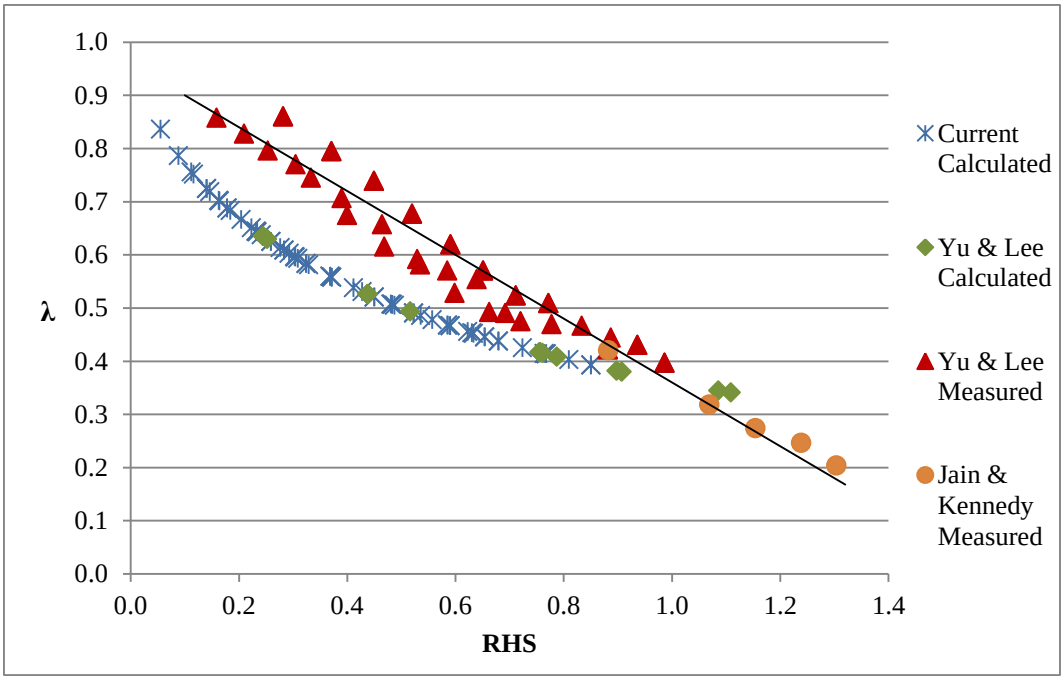


Figure 4-1: Yu and Lee data vs. results for air core ratio formula

Comparisons were made between the air concentration and the air core using various combinations of air core diameter, drop shaft length and air core volume. These relationships show that there is no direct correlation between the variables alone. The air discharge was also compared to the air core diameter divided by the drop shaft length as well as the air core volume. The results were similarly inconclusive.

### 4.2. Air core ratio analysis

The air core diameter ratio ($\lambda$) was compared directly to the air concentration. This showed a common trend between the different drop shafts, but no definable relationship. The air core ratio was combined with the air core area divided by the length of the drop shaft. Like the previous comparison, a common trend was observed, but no quantifiable relationship.

### 4.3. Jet velocity analysis

The velocities for the tangential and vertical components were computed using Equations 1-11 and 1-12 from Jain (1984). From these component velocities, a jet velocity vector was calculated to determine the stream wise velocity of the water located at the throat of the air-core. The jet velocity was plotted against the air discharge and showed an agreeable correlation between the two. The air discharge was then divided by the drop shaft length, air core diameter and $\lambda$ and plotted against the jet velocity. This showed two distinct trends that suggest another variable could combine the trends. The drop shaft diameter was substituted for the air core diameter and the results were similar.

The terminal velocity was calculated using Equation 1-8 suggested by Jain (2004). The terminal velocity was substituted for the jet velocity and plotted against the air discharge divided by the drop shaft length, diameter, and the air core ratio. This showed an excellent trend for all the data. The diameter of the air core replaced the drop shaft diameter and the data collapsed closer to the trend line with an $R^2$ value of 0.775. The data would prove much better without the presence of the AS6 data which follows the trend until about 4 m/s and then jumps to higher values with roughly the same trend.

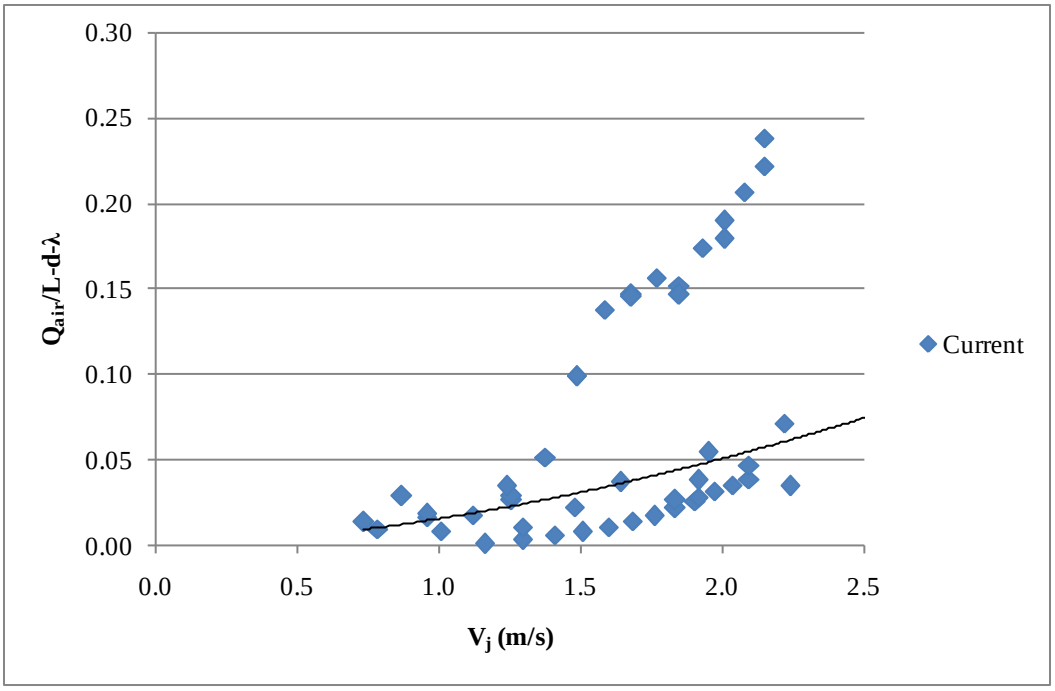


Figure 4-2: Air discharge relationship with calculated jet velocity

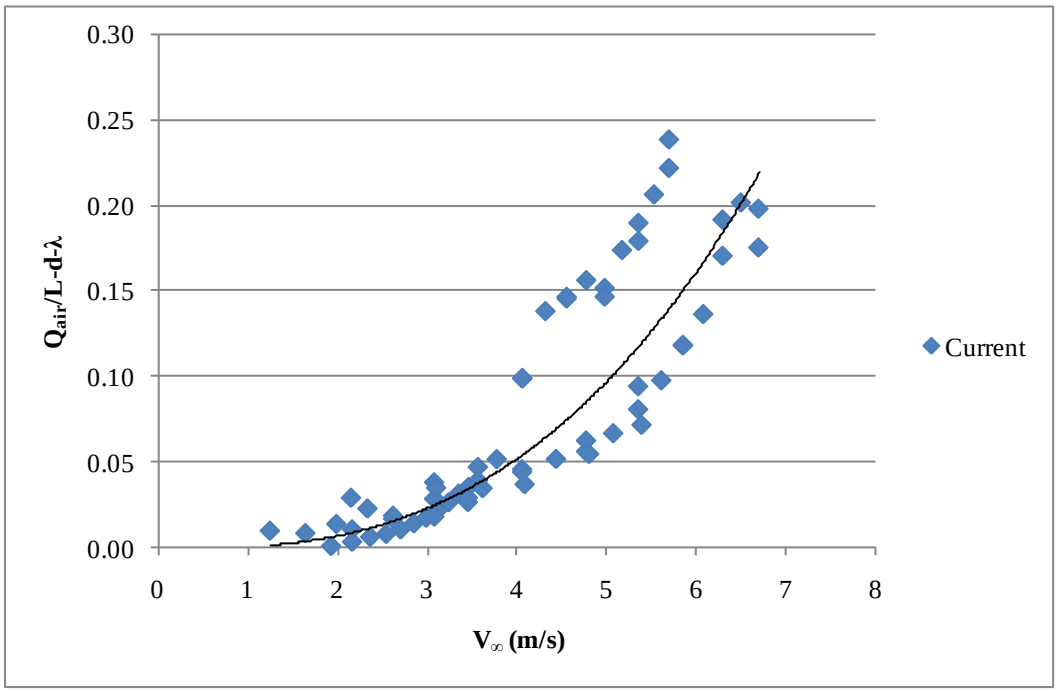


Figure 4-3: Terminal jet velocity vs. air discharge

This relationship is similar to the trend found by Zhao (2006). Using the jet velocity plotted against air discharge over jet thickness (W=$\pi$*$D$), Zhao showed an increasing trend of air discharge with increasing velocity. Data was taken from Zhao's plot and compared with current jet velocity and air discharge in the same manner. The comparison is shown in Figure 4-4. This relationship has much scatter and uses a coefficient to manipulate data by each drop shaft, if needed, to obtain a better fit. This coefficient is considered impractical for the purpose of this study but nonetheless shows a correlation between previous studies of vortex drop shafts and the current one.

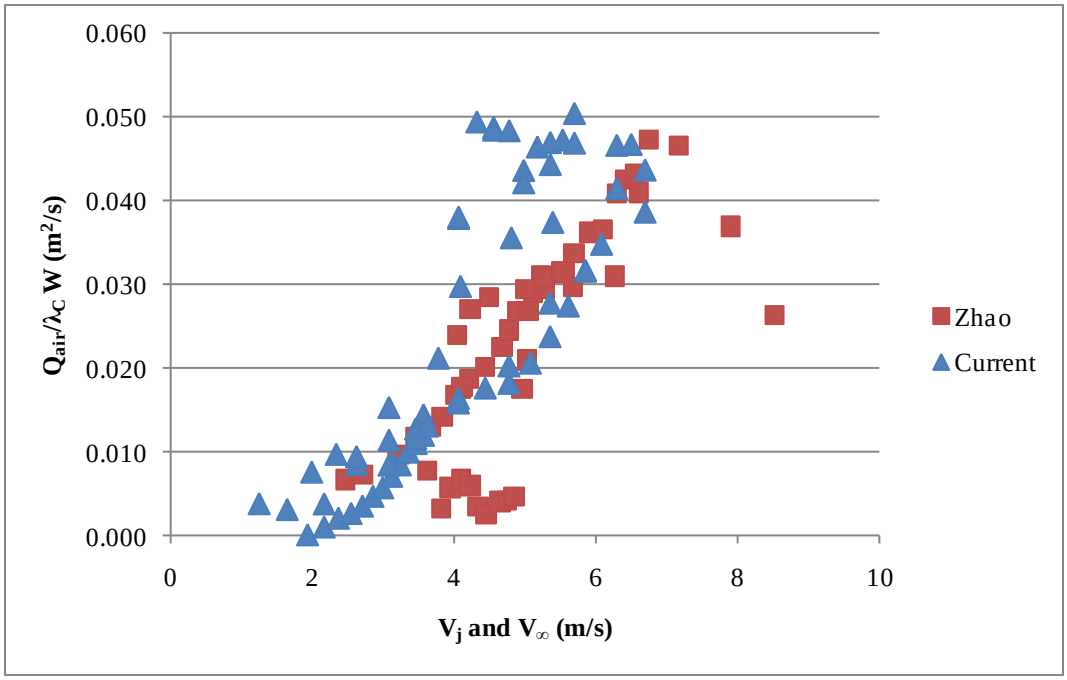


Figure 4-4: Zhao data with current data

### 4.4. Dimensionless analysis

Many dimensionless relationships were developed using simple unit cancellations between variable that are considered to be responsible for the air entrainment rate. The air core ratio and drop shaft length were commonly used as base variables to build a

probable relationship. The air concentration was used often in the same manner. Trying various combinations of lambda, drop shaft length, air core diameter and drop shaft diameter to obtain a dimensionless parameter, the calculations were plotted against the air concentration or a new dimensionless version of air discharge. This approach showed many plots with tremendous scatter among the data with no leads towards a direct relationship. The terminal velocity was also derived into a dimensionless form using the drop shaft length, water discharge, and drop shaft diameter to obtain:

$$V_{\infty}^{*} = \frac{L}{\pi^{2/5}}\left(\frac{D}{nQ_w}\right)^{3/5} \tag{4-2}$$

While the dimensionless terminal velocity showed a trend against the air concentration, the scatter of the data was too great for a good relationship.

### 4.5. Froude number analysis

From the dimensionless analysis, a Froude number approach was developed. The velocity of the jet was introduced with gravity on both axes of the plots to attempt to obtain a definite correlation. The Froude number of the water was calculated using the jet velocity at the throat of the air core and the depth of the water against the drop shaft wall at the throat of the air core. While this did not give a usable relationship, a trend in some of the data could be seen.

The Froude number was calculated using the terminal velocity as well. Plotting against the air concentration, both types of Froude numbers showed a small trend but still lacking in confidence. The Froude number was multiplied with the air core ratio as well but with less success than other attempts. The Froude number analysis does show a trend towards an air concentration of roughly 0.5 when the Froude number is above 1.0 or super critical flow.

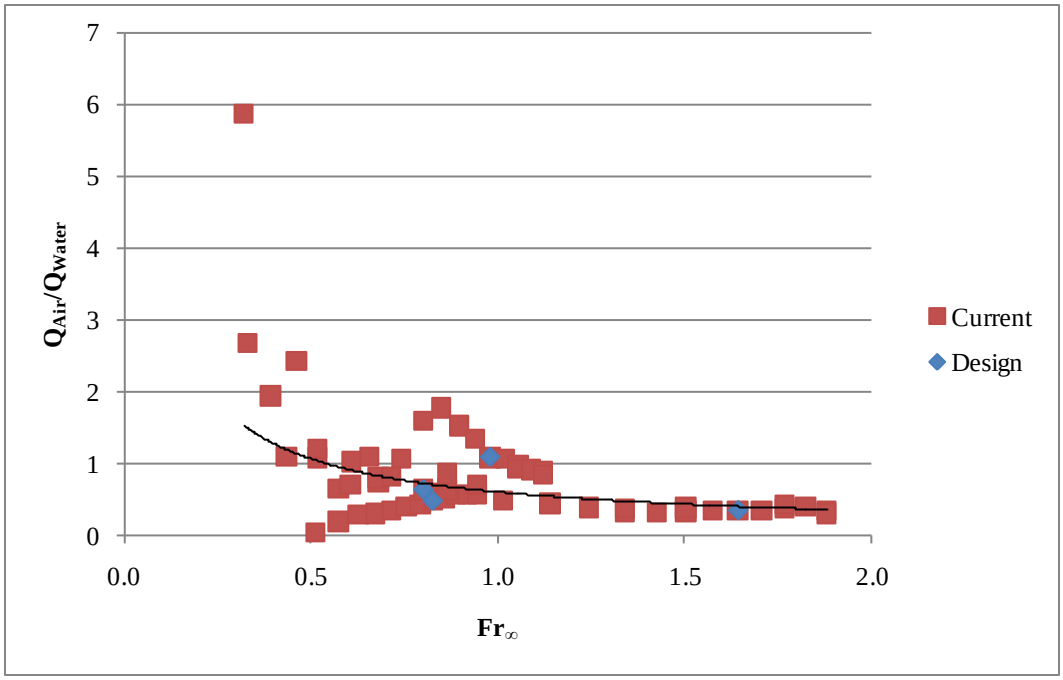


Figure 4-5: Air concentration vs. Froude number of terminal velocity

### 4.6. Dimensional analysis

Applying the theory known as the *X*-parameter with multi-variables and exponents showed a much more promising trend. The *X*-parameter consists of the length of a jet in contact with air before plunging, the diameter of the jet, and the velocity of the jet. Various combinations of diameters and velocities were experimented with the parameter. The drop shaft diameter combined with the terminal velocity and drop shaft length showed a good trend with the data. The air core diameter was tried and gave even better results. The data was compared to data extracted from 2 figures from Bin (1993) and is nearly on the same trend line. The data is an order of magnitude greater than the jet nozzle data with slightly different coefficients for the power law relationship.

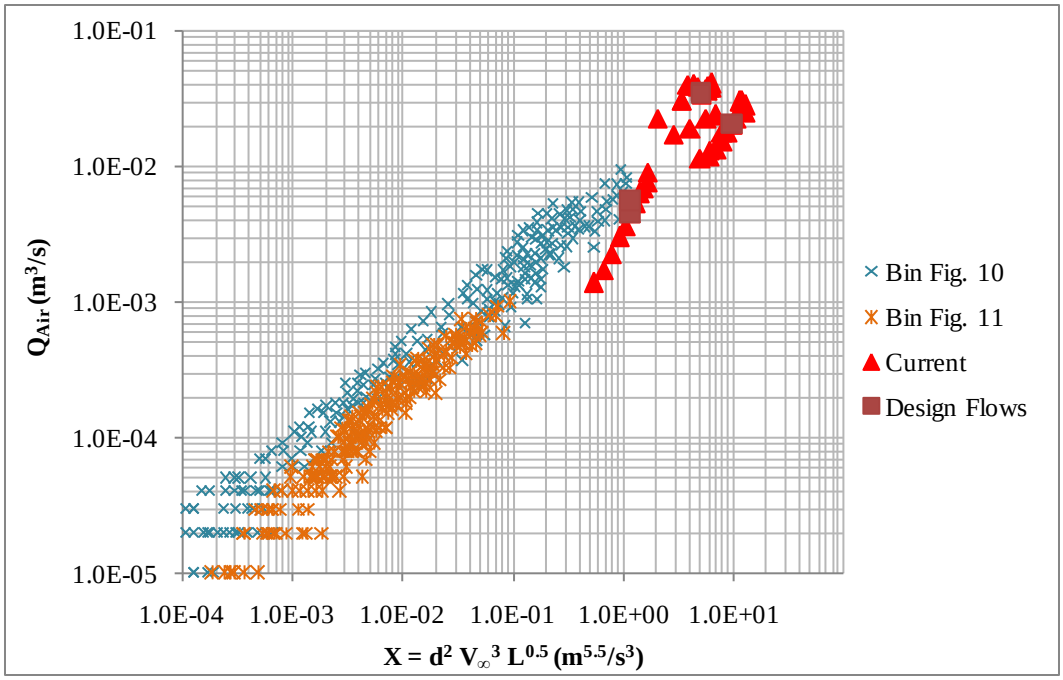


Figure 4-6: *X* parameter with air core diameter

A new concept was also explored in which the equivalent diameter ($d_e$) was calculated from the air core. Using the width of the jet against the wall of the drop shaft, the cross sectional area of the water was translated from a ring to a circle. The diameter of the circle calculated was then used as a representative for a plunging jet.

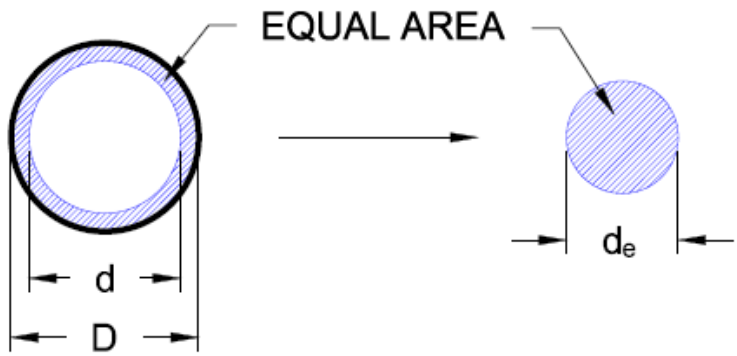


Figure 4-7: Equivalent diameter

The equivalent diameter was substituted in for the air core diameter in the X parameter. The results gave more scatter of the data but showed a better slope in comparison to the Sande and Smith data. The Bin data was then also compared to both sets and fit the scatter wonderfully.

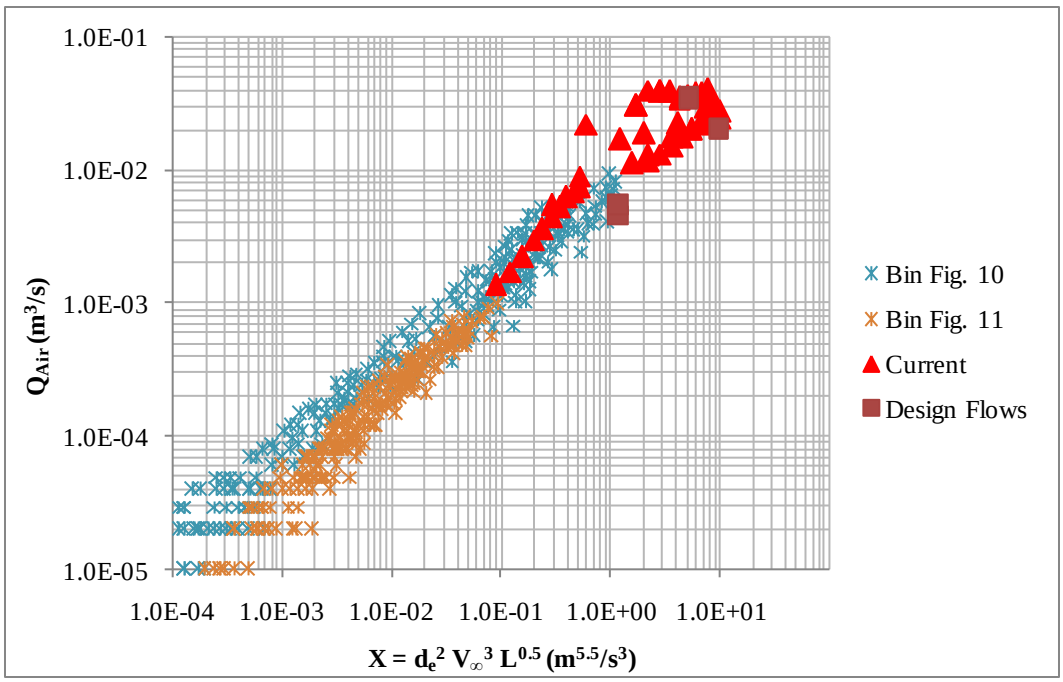


Figure 4-8: *X* parameter relationship with equivalent diameter

Using data from water flows greater than 40% of the design flow, the plot shows scatter among relationship. Adding in the 40% design flows, the scatter becomes more scattered. Using only the 100% design flows, the trend fits nearly perfect to the Bin data.

### 4.7. Uncertainty analysis

An analysis of possible errors in data collection was done to determine the uncertainty of the data before analysis. The first possible error comes from the instrumentation. The hot wire anemometers have a factory error of up to 2% (or ±1%)

for the range of velocities they were used for. Other factory errors for environmental conditions such as temperature and humidity are considered negligible since the calibration error accounts for the environment.

The second possible error is the calibration error of the instrument. The hot wire anemometers were calibrated in-situ to determine the accurate slope and intercept to translate voltage into velocity. This calibration has a different slope than the factory setting. The difference from factory to in-situ can be considered a possible error in the data collection process. The checking of the calibration assures that the in-situ is correctly translating the data for the environment the instrument is in, however it must be considered in the error analysis. The calibrations for each hot wire anemometer were different, so an average error was calculated to represent them. The average error was 2.8%.

A third error is the precision of the data collection. A moving average determines the time required for the average of the data to stabilize. From the time required, a sample time is established. Every time the sample time is reached during the data collection, the data is considered an individual sample. The data was typically collected for 60 seconds and the sample time was determined to be 20 seconds. Thus, there were 3 samples per data collection. Some data collection was acquired for 300 seconds in which case there were 15 samples per collection. Using a t-student distribution with a 95% confidence level, the precision limit was found for a 300 second collection. Using a value of 2 for the coverage factor, the precision limit was calculated to be relatively small. The precision limit was found to have an error of 1.1% when compared to the accepted value or average of the collection.

For all errors in the equations used, the error was considered indeterminate since there is no error analysis for most of the empirical and analytical formulas. All error from these formulas must be considered an integral part of the studies themselves.

Once the main sources of error in the data collection were determined, an overall error combining the sources was determined to be 3.6%.

# CHAPTER 5. AIR ENTRAINMENT RELATIONSHIP

## 5.1. Best fit relationship

The best fit for the data collected is the X parameter vs. the air discharge. With a sum of squares value of 0.9532, the exponential relationship using the new linear air core diameter method and terminal velocity has a slightly better fit than the equivalent diameter. However the *X* parameter with the equivalent diameter has a slope and coefficient closer to that of the Bin data. The equation of the best fit line, shown in Figure 5-1 is: $Q_a = 0.0078X^{0.7338}$, where the coefficient and exponent from Bin are 0.0076 and 0.75, respectively.

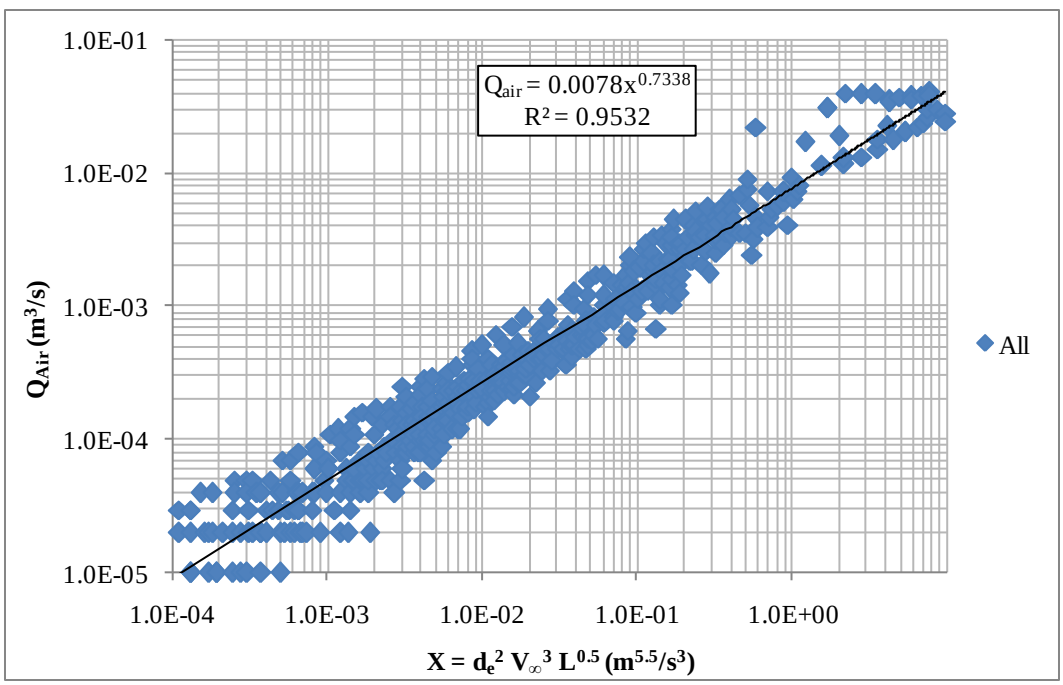


Figure 5-1: Best fit relationship

A standard deviation analysis of the best fit relationship was performed to determine the accuracy of using this method. Figure 5-2 shows the results.

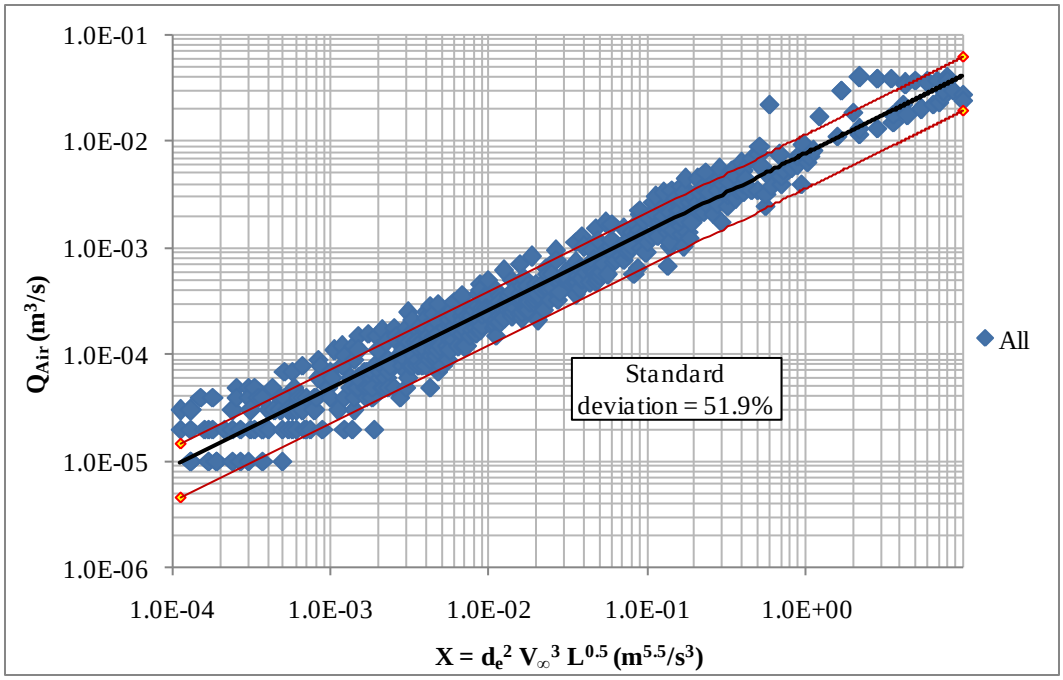


Figure 5-2: Standard deviations for best fit relationship

The standard deviation is given as a percentage due to the nature of the logarithmic plot. A linear standard deviation is not possible in terms of a dimensional value of $Q_{air}$. The values of $Q_{air}$ were taken as a percentage different from the best fit line and then a standard deviation calculation was performed on the percentages. An overall standard deviation was determined to be 51.9%.

The next best fit relationship is the terminal velocity plotted against the air discharge divided by the drop shaft length, diameter, and the air core ratio, shown in Figure 4-3. The plot shows that $V_\infty \propto Q_{air}/(Ld\lambda)$ and when fit with an exponential relationship the empirical equation becomes:

$$\frac{Q_{air}}{Ld\lambda} = 0.001V_\infty^{2.76} \tag{5-1}$$

The relationship has a sum of squares value of 0.775. Had the AS6 drop shaft data not been used, the relationship would have proven much better. The data shows a split in the relationship for AS6 around a terminal velocity of 4 m/s.

### 5.2. Scaling Effects

The air entrainment relationships are based on model scale measurements and therefore needs scaling for use upon prototype designs. Scaling is still an unconfident issue for air discharge. The scaling law says to multiply by the scale ratio to a power of 2.5. However it was determined that scaling alone will under estimate the flow by a factor between 2 and 4 according to Ervine and Kolkman (1980).

The Jain and Kennedy (1983) study of vortex flow drop structures included an estimate of the factor of underestimation. The estimate was obtained by comparing flow characteristics in two models of different scales, a “small-scale” model and a “large-scale” model. The large-scale model was 2.3 times larger than the small-scale model. The comparison shows that airflow rates do not scale according to this law. The results suggest that airflow rates that are scaled according to Froude’s law must be multiplied by an additional scaling factor equal to the prototype to model ratio raised to a power of 0.34. For the ADDS model, the prototype to model ratio is 7, so the additional scaling factor is $7^{0.34} = 1.94$.

Another concern is not knowing what the scale should be before any design work is done. This study should merely be used for an approximation of the air discharge of model scale vortex drop shafts. Once this study has been tested among other applications and against prototype values, a more accurate prediction method can be developed.

### 5.3. Example of application

The process of determining air discharge for a model should be done as described in the following paragraphs. All units are in SI, and all lengths are used as meters.

For a model scale vortex drop shaft, once the geometry is designed according to typical criteria, the right-hand side of the Yu and Lee (2009) formula, Equation 1-10, should be solved for the design water discharge. The air core ratio can then be solved using iterations or a solver. Alternatively, a much easier to solve, but unproven method of using the linear relationship of Yu and Lee's data: $\lambda = -0.6*RHS+0.96$ could be used. The diameter of the air core is determined from $\lambda = d^2/D^2$ to serve as the jet diameter. The terminal velocity of the water inside the drop shaft is then calculated using Jain's (2004) Equation 1-8 with water discharge and drop shaft diameter. The roughness is the Manning roughness. The length of the drop shaft in this study is considered to be from the bottom of the tangential inlet to the top of the adit or de-aeration chamber. Using Figure 4-3, the air discharge can be determined with the calculated variables.

To use the recommended $X$ parameter method, the water area can be solved for from the diameter using $A = \pi*(D^2-d^2)/4$. The equivalent diameter of the water area is then calculated by assuming a circle for the area, rather than a ring. The $X$ parameter can now be solved with the equivalent diameter, terminal velocity and length of the drop shaft where $X = d_e^2\ V_\infty^3\ L^{0.5}$. The air discharge can now be read from Figure 4-8 or calculated with the relationship: $Q_a = 0.0078X^{0.7338}$. The discharge also has a standard deviation of roughly 51.9% that must be taken into consideration for any practical purposes.

# CONCLUSION

The dimensional analysis of the vortex drop shaft structure is currently the best theory for predicting the air discharge. The quantity of air is best determined using an exponential relationship of terminal velocity, air core diameter and drop shaft length with individual exponents to create the *X* parameter that is also multiplied by a coefficient and raised to a given power.

Ultimately, the geometry of the inlet and outlet will change the amount of air that will be entrained. This study attempted to incorporate the different types of geometric configurations that are common among current drop shafts. The results show the complexity of the relationship.

The uncertainty of the data collection and analysis was determined to be roughly 3.6%. The errors inquired during testing were considered to be acceptable for this study. The largest error in this study is the use of empirical equations and relationships between them. The standard deviation of the best fit relationship was roughly 51.9% that must be accounted for in any practical application of the best fit method.

The scaling of model to prototype of air discharge in drop shafts is still considered approximate at best. More research is needed to determine the correct relationship of air entrainment when scaling.

Further studies are also needed to determine a better relationship for air entrainment at any scale. The study done here only incorporates model scale data. There is very little data collected from prototype scale drop shafts, if any. The relationships found here are empirical and may not represent all geometries of vortex drop structures. A suggestion of using a scale of 1:4 or less for a model in comparison with a smaller scale model of 1:10 would be desirable for determining a good scaling relationship for air entrainment.

# REFERENCES


Ahmed, A. "Aeration by Plunging Liquid Jet." Ph.D. Thesis. Loughborough University of Technology, 1974.

Bagatur, Tamer, and Nusret Sekerdag." Air-Entrainment Characteristics in a Plunging Water Jet System Using Rectangular Nozzles with Rounded Ends."*Water SA* 29.1 (2003): 35-38. *Water Research Commission*. Web.<www.wrc.org.za>.

Bin, Andrezej K. "Gas Entrainment by Plunging Liquid Jets." *Chemical Engineering Science* 48.21 (1993): 3385-630. Print.

Chanson, H., and R. Manasseh."Air Entrainment Processes in a Circular Plunging Jet: Void-Fraction and Acoustic Measurements." *Journal of Fluids Engineering* 125.5 (2003): 910-21. Print.

Chanson, H., and T. Brattberg."Air Entrainment by Two-Dimensional Plunging Jets: The Impingement Region and the Very-Near Flow Field." *ASME*. Proc. of ASME Fluids Engineering Division Summer Meeting, Washington, DC.June 1998.Web.

Chanson, H. "Turbulent Air–Water Flows in Hydraulic Structures: Dynamic Similarity and Scale Effects." *Environmental Fluid Mechanics* 9.2 (2008): 125-42. Print.

Cumming, I. W. "The Impact of Falling Liquids with Liquid Surfaces." Ph.D. Thesis. Loughborough University of Technology., 1975.

Deswal, Surinder. "Oxygenation by Hollow Plunging Water Jet." *Journal of the Institute of Engineering* 7.1 (2009): 1-8. Print.

Ervine, D. A., E. J. McKeogh, and E. M. Elsawy. "Effect of Turbulence Intensity on the Rate of Air Entrainment by Plunging Water Jets." *Pruc. Instn Civil Engrs* Part 2, 69 (1980): 425-45.

Funatsu, K., Y.-Ch. Hsu, and T. Kamogawa. "Gas Holdup and Gas Entrainment of a Plunging Water Jet with a Constant Entrainment Guide." *Can. J. Chem. Engng* 66 (1988): 19-28.

Gualtieri, Paola, and Guelfo Pulci Doria."Air Entrainment in Vertical Drop Shafts: A New Hydrodynamic Model." *Advances in Hydro-Science and Engineering* VI (2006): 1-10.

Jain, Subhash C., and J. F. Kennedy. *Vortex-Flow Drop Structures for the Milwaukee Metropolitan Sewerage District Inline Storage System*. IIHR Report No. 264. Iowa City, Iowa: Iowa Institute of Hydraulic Research, The University of Iowa, 1983. Print.

Jain, Subhash C. *Hydraulic Design of Drop Structures for the West Area CSO Storage Tunnel Atlanta, Georgia*. IIHR Limited Distribution Report No. 319. Iowa City, Iowa: IIHR – Hydroscience & Engineering, The University of Iowa, 2004. Print.

Jain, Subhash C. "Tangential Vortex-Inlet." *Journal of Hydraulic Engineering* 110.12 (1984): 1693-699. *ASCE*. Web.

Kumagai, M., and H. Imai. "Gas Entrainment Phenomena and Flow Pattern of an Impinging Water Jet." *Kagaku Kagaku Ronbunshu* 8 (1982): 510-13.

Luca, Ciaravino, Paola Gualtieri, and Guelfo Pulci Doria."Air Entrainment in Central Jet Drop Shafts: Theoretical Formulation and Experimental Implementation." (2008). Print.

Lyons, Troy C., and A. Jacob Odgaard. *Hydraulic Model Study for the City Of Indianapolis' Deep Rock Tunnel Connector Drop Structures*. Limited Distribution Report No. 370 Iowa City, Iowa: IIHR – Hydroscience & Engineering, The University of Iowa, 2010. Print.

Lyons, Troy C., Marian Muste, Andy J. Craig, and A. Jacob Odgaard. *Hydraulic Model Studies for Drop Structures: Abu Dhabi Strategic Tunnel Enhancement Programme (STEP)*. Limited Distribution Report No. 371. Iowa City, Iowa: IIHR – Hydroscience & Engineering, The University of Iowa, 2010. Print.

McKeogh, E. J., and D. A. Ervine."Air Entrainment Rate and Diffusion Pattern of Plunging Liquid Jets." *Chemical Engineering Science* 36 (1981): 1161-172. Print.

Ohkawa, A., D. Kusabiraki, Y. Shiokawa, N. Sakai, and M. Fujii. "Flow and Oxygen Transfer in a Plunging Water System Using Inclined Short Nozzles and Performance Characteristics of Its System in Aerobic Treatment of Wastewater." *Biotechnol. Bioengng* 88 (1986): 1845-856.

Ohkawa, A., D. Kusabiraki, and N. Sakai. "Effect of Nozzle Length on Gas Entrainment Characteristics of Vertical Liquid Jet." *J. Chem. Engng Japan* 20 (1987): 295-300.

Rajaratnam, N., A. Mainali, and C. Y. Hsung." Observations on Flow in Vertical Drop Shafts in Urban Drainage Systems." *Journal of Environmental Engineering* 123.5 (1997): 486-91. *ASCE*. Web.

Schmidtke, M., and D. Lucas."On The Modeling of Bubble Entrainment by Impinging Jets in CFS-Simulations." 2008. Web.

Smit, Arnout. "Air Entrainment with Plunging Jets." Thesis. Delft University of Technology, 2007.Print.

Toda, K., and K. Inoue." Hydraulic Design of Intake Structures of Deeply Located Underground Tunnel Systems." *Wat. Sci. Tech.* 39.9 (1999): 137-44. Print.

Van De Sande, E., and John M. Smith." Jet Break-Up and Air Entrainment by Low Velocity Turbulent Water Jets." *Chemical Engineering Science* 31 (1976): 219-24. Print.

Yu, Daeyoung, and Joseph H. W. Lee." Hydraulics of Tangential Vortex Intake for Urban Drainage." *Journal of Hydraulic Engineering © ASCE* 135.3 (2009): 164-74. Web.

Zhao, Can-Hua, David Z. Zhu, Shuang-Ke Sun, and Zhi-Ping Liu. "Experimental Study of Flow in a Vortex Drop Shaft." *Journal of Hydraulic Engineering © ASCE* January (2006): 61-68. Web.

# APPENDIX – DATA

| Drop Shaft | L (m) | D (m) | e (m) | β (°) | % $Q_{Design}$ | $Q_{Water}$ ($m^3/s$) | $Q_{Air}$ ($m^3/s$) | $Q_{Air}$ / $Q_{Water}$ | RHS | λ | d (m) |
|---|---|---|---|---|---|---|---|---|---|---|---|
| MPS1 | 1.454 | 0.200 | 0.032 | 27.5 | 10% | 0.00092 | 0.00247 | 2.686 | 0.0559 | 0.926 | 0.193 |
| | | | | | 20% | 0.00184 | 0.00203 | 1.107 | 0.0888 | 0.907 | 0.190 |
| | | | | | 30% | 0.00276 | 0.00014 | 0.052 | 0.1164 | 0.890 | 0.189 |
| | | | | | 40% | 0.00367 | 0.00073 | 0.198 | 0.1410 | 0.875 | 0.187 |
| | | | | | 50% | 0.00459 | 0.00138 | 0.301 | 0.1636 | 0.862 | 0.186 |
| | | | | | 60% | 0.00551 | 0.00174 | 0.316 | 0.1847 | 0.849 | 0.184 |
| | | | | | 70% | 0.00643 | 0.00229 | 0.356 | 0.2047 | 0.837 | 0.183 |
| | | | | | 80% | 0.00735 | 0.00302 | 0.411 | 0.2238 | 0.826 | 0.182 |
| | | | | | 90% | 0.00827 | 0.00366 | 0.442 | 0.2421 | 0.815 | 0.181 |
| | | | | | 100% | 0.00919 | 0.00452 | 0.492 | 0.2597 | 0.804 | 0.179 |
| | | | | | 110% | 0.01011 | 0.00537 | 0.531 | 0.2767 | 0.794 | 0.178 |
| | | | | | 120% | 0.01102 | 0.00632 | 0.574 | 0.2932 | 0.784 | 0.177 |
| | | | | | 130% | 0.01194 | 0.00696 | 0.583 | 0.3093 | 0.774 | 0.176 |
| | | | | | 140% | 0.01286 | 0.00758 | 0.589 | 0.3250 | 0.765 | 0.175 |
| AS6 | 2.642 | 0.216 | 0.052 | 35.0 | 10% | 0.00320 | 0.00626 | 1.952 | 0.1465 | 0.872 | 0.202 |
| | | | | | 20% | 0.00641 | 0.00700 | 1.092 | 0.2326 | 0.820 | 0.196 |
| | | | | | 30% | 0.00961 | 0.00694 | 0.721 | 0.3047 | 0.777 | 0.190 |
| | | | | | 40% | 0.01282 | 0.00951 | 0.742 | 0.3692 | 0.738 | 0.186 |
| | | | | | 50% | 0.01602 | 0.01728 | 1.079 | 0.4284 | 0.703 | 0.181 |
| | | | | | 60% | 0.01923 | 0.03081 | 1.602 | 0.4838 | 0.670 | 0.177 |
| | | | | | 70% | 0.02243 | 0.04016 | 1.790 | 0.5361 | 0.638 | 0.172 |
| | | | | | 80% | 0.02564 | 0.03963 | 1.545 | 0.5860 | 0.608 | 0.168 |
| | | | | | 90% | 0.02884 | 0.03931 | 1.363 | 0.6339 | 0.580 | 0.164 |
| | | | | | 100% | 0.03205 | 0.03546 | 1.106 | 0.6800 | 0.552 | 0.160 |
| | | | | | 110% | 0.03525 | 0.03773 | 1.070 | 0.7246 | 0.525 | 0.156 |
| | | | | | 120% | 0.03846 | 0.03817 | 0.992 | 0.7679 | 0.499 | 0.153 |
| | | | | | 130% | 0.04166 | 0.03841 | 0.922 | 0.8100 | 0.474 | 0.149 |
| | | | | | 140% | 0.04487 | 0.04098 | 0.913 | 0.8510 | 0.449 | 0.145 |
| WS6 | 1.296 | 0.257 | 0.057 | 27.5 | 10% | 0.00572 | 0.00634 | 1.108 | 0.1127 | 0.892 | 0.243 |
| | | | | | 20% | 0.01144 | 0.00741 | 0.648 | 0.1790 | 0.853 | 0.237 |
| | | | | | 30% | 0.01715 | 0.00851 | 0.496 | 0.2345 | 0.819 | 0.233 |
| | | | | | 40% | 0.02287 | 0.01063 | 0.465 | 0.2840 | 0.790 | 0.229 |
| | | | | | 50% | 0.02859 | 0.01143 | 0.400 | 0.3296 | 0.762 | 0.225 |
| | | | | | 60% | 0.03431 | 0.01179 | 0.344 | 0.3722 | 0.737 | 0.221 |
| | | | | | 70% | 0.04003 | 0.01335 | 0.334 | 0.4124 | 0.713 | 0.217 |
| | | | | | 80% | 0.04574 | 0.01538 | 0.336 | 0.4508 | 0.690 | 0.214 |
| | | | | | 90% | 0.05146 | 0.01773 | 0.345 | 0.4877 | 0.667 | 0.210 |
| | | | | | 100% | 0.05718 | 0.02048 | 0.358 | 0.5232 | 0.646 | 0.207 |
| | | | | | 110% | 0.06290 | 0.02248 | 0.357 | 0.5575 | 0.626 | 0.203 |
| | | | | | 120% | 0.06862 | 0.02677 | 0.390 | 0.5908 | 0.606 | 0.200 |
| | | | | | 130% | 0.07434 | 0.03016 | 0.406 | 0.6232 | 0.586 | 0.197 |
| | | | | | 140% | 0.08005 | 0.02819 | 0.352 | 0.6547 | 0.567 | 0.194 |
| INDY | 4.629 | 0.203 | 0.051 | 28.0 | 10% | 0.00368 | 0.02165 | 5.886 | 0.1647 | 0.861 | 0.189 |
| | | | | | 25% | 0.00920 | 0.02238 | 2.433 | 0.3033 | 0.778 | 0.179 |
| | | | | | 50% | 0.01840 | 0.01901 | 1.033 | 0.4815 | 0.671 | 0.166 |
| | | | | | 75% | 0.02759 | 0.02270 | 0.823 | 0.6310 | 0.581 | 0.155 |
| | | | | | 100% | 0.03679 | 0.02387 | 0.649 | 0.7644 | 0.501 | 0.144 |

Data Extracted from Bin (1993) Fig. 10

| X | Qa | X | Qa | X | Qa | X | Qa | X | Qa |
|---|---|---|---|---|---|---|---|---|---|
| 0.00013 | 0.00001 | 0.22623 | 0.00222 | 0.01222 | 0.00062 | 0.00121 | 0.00010 | 0.13237 | 0.00145 |
| 0.00013 | 0.00001 | 0.26220 | 0.00208 | 0.00979 | 0.00051 | 0.00138 | 0.00009 | 0.11631 | 0.00133 |
| 0.00017 | 0.00001 | 0.29283 | 0.00177 | 0.00860 | 0.00046 | 0.00193 | 0.00015 | 0.11013 | 0.00218 |
| 0.00019 | 0.00001 | 0.31546 | 0.00254 | 0.00860 | 0.00041 | 0.00200 | 0.00011 | 0.09499 | 0.00182 |
| 0.00021 | 0.00002 | 0.35905 | 0.00291 | 0.00676 | 0.00035 | 0.00223 | 0.00013 | 0.10418 | 0.00195 |
| 0.00024 | 0.00002 | 0.40120 | 0.00340 | 0.00605 | 0.00032 | 0.00149 | 0.00011 | 0.13744 | 0.00223 |
| 0.00031 | 0.00002 | 0.54879 | 0.00248 | 0.00467 | 0.00030 | 0.00254 | 0.00015 | 0.13239 | 0.00162 |
| 0.00027 | 0.00002 | 0.55926 | 0.00325 | 0.00418 | 0.00029 | 0.00294 | 0.00018 | 0.11211 | 0.00142 |
| 0.00033 | 0.00002 | 0.60229 | 0.00389 | 0.00396 | 0.00025 | 0.00317 | 0.00016 | 0.10605 | 0.00130 |
| 0.00044 | 0.00003 | 0.69816 | 0.00398 | 0.00323 | 0.00021 | 0.00361 | 0.00019 | 0.12762 | 0.00182 |
| 0.00040 | 0.00002 | 0.93805 | 0.00407 | 0.00306 | 0.00025 | 0.00396 | 0.00022 | 0.12764 | 0.00203 |
| 0.00049 | 0.00002 | 0.71137 | 0.00476 | 0.00249 | 0.00018 | 0.00476 | 0.00020 | 0.12535 | 0.00249 |
| 0.00067 | 0.00002 | 0.72479 | 0.00545 | 0.00207 | 0.00017 | 0.00450 | 0.00024 | 0.15081 | 0.00298 |
| 0.00056 | 0.00003 | 0.80973 | 0.00570 | 0.00169 | 0.00016 | 0.00542 | 0.00024 | 0.15932 | 0.00227 |
| 0.00051 | 0.00004 | 0.88811 | 0.00610 | 0.00146 | 0.00015 | 0.00573 | 0.00027 | 0.14523 | 0.00186 |
| 0.00065 | 0.00004 | 1.01067 | 0.00638 | 0.00141 | 0.00012 | 0.00769 | 0.00028 | 0.16522 | 0.00162 |
| 0.00160 | 0.00007 | 1.06849 | 0.00746 | 0.00117 | 0.00012 | 0.00701 | 0.00025 | 0.14788 | 0.00148 |
| 0.00079 | 0.00004 | 1.10884 | 0.00816 | 0.00105 | 0.00011 | 0.00926 | 0.00034 | 0.16527 | 0.00194 |
| 0.00101 | 0.00006 | 0.97466 | 0.00935 | 0.00082 | 0.00009 | 0.00844 | 0.00037 | 0.18464 | 0.00208 |
| 0.00130 | 0.00006 | 0.88837 | 0.00730 | 0.00065 | 0.00008 | 0.00892 | 0.00028 | 0.18820 | 0.00305 |
| 0.00185 | 0.00008 | 0.68610 | 0.00747 | 0.00057 | 0.00007 | 0.01155 | 0.00036 | 0.16537 | 0.00285 |
| 0.00231 | 0.00009 | 0.52965 | 0.00584 | 0.00051 | 0.00007 | 0.01093 | 0.00041 | 0.16850 | 0.00333 |
| 0.00268 | 0.00013 | 0.40150 | 0.00534 | 0.00042 | 0.00005 | 0.01390 | 0.00051 | 0.16545 | 0.00382 |
| 0.00300 | 0.00014 | 0.34638 | 0.00534 | 0.00033 | 0.00005 | 0.01672 | 0.00053 | 0.20636 | 0.00272 |
| 0.00354 | 0.00017 | 0.27240 | 0.00436 | 0.00030 | 0.00005 | 0.01611 | 0.00044 | 0.20255 | 0.00243 |
| 0.00403 | 0.00018 | 0.23507 | 0.00523 | 0.00030 | 0.00004 | 0.02375 | 0.00058 | 0.21027 | 0.00333 |
| 0.00450 | 0.00018 | 0.23068 | 0.00408 | 0.00025 | 0.00005 | 0.03132 | 0.00052 | 0.27723 | 0.00260 |
| 0.00594 | 0.00019 | 0.20653 | 0.00447 | 0.00025 | 0.00004 | 0.04789 | 0.00057 | 0.32146 | 0.00318 |
| 0.00741 | 0.00023 | 0.17172 | 0.00447 | 0.00024 | 0.00003 | 0.04056 | 0.00059 | 0.23492 | 0.00349 |
| 0.00978 | 0.00024 | 0.14272 | 0.00349 | 0.00018 | 0.00004 | 0.03436 | 0.00065 | 0.27737 | 0.00348 |
| 0.01364 | 0.00035 | 0.12541 | 0.00334 | 0.00015 | 0.00004 | 0.04703 | 0.00072 | 0.24827 | 0.00333 |
| 0.01701 | 0.00027 | 0.11225 | 0.00305 | 0.00013 | 0.00003 | 0.05159 | 0.00085 | 0.23052 | 0.00266 |
| 0.02047 | 0.00037 | 0.11017 | 0.00273 | 0.00011 | 0.00003 | 0.04452 | 0.00097 | 0.21405 | 0.00222 |
| 0.02374 | 0.00041 | 0.08346 | 0.00170 | 0.00011 | 0.00002 | 0.03913 | 0.00104 | 0.18472 | 0.00266 |
| 0.02752 | 0.00046 | 0.08991 | 0.00233 | 0.00013 | 0.00002 | 0.04795 | 0.00122 | 0.30426 | 0.00408 |
| 0.03497 | 0.00037 | 0.08825 | 0.00208 | 0.00013 | 0.00003 | 0.06092 | 0.00087 | 0.32150 | 0.00348 |
| 0.03837 | 0.00052 | 0.07068 | 0.00152 | 0.00017 | 0.00002 | 0.07063 | 0.00099 | 0.33369 | 0.00417 |
| 0.04788 | 0.00051 | 0.05987 | 0.00170 | 0.00018 | 0.00002 | 0.05984 | 0.00121 | 0.31577 | 0.00467 |
| 0.05551 | 0.00057 | 0.05360 | 0.00174 | 0.00016 | 0.00002 | 0.07603 | 0.00095 | 0.35934 | 0.00477 |
| 0.06090 | 0.00076 | 0.04709 | 0.00156 | 0.00031 | 0.00003 | 0.06932 | 0.00085 | 0.36586 | 0.00356 |
| 0.08647 | 0.00066 | 0.05982 | 0.00104 | 0.00037 | 0.00004 | 0.08038 | 0.00106 | 0.41649 | 0.00456 |
| 0.09845 | 0.00091 | 0.03843 | 0.00133 | 0.00048 | 0.00004 | 0.07330 | 0.00116 | 0.40878 | 0.00398 |
| 0.13221 | 0.00069 | 0.03568 | 0.00114 | 0.00058 | 0.00005 | 0.07895 | 0.00145 | 0.58064 | 0.00466 |
| 0.13727 | 0.00104 | 0.02607 | 0.00095 | 0.00062 | 0.00004 | 0.09150 | 0.00133 | 0.45657 | 0.00356 |
| 0.16817 | 0.00103 | 0.02654 | 0.00079 | 0.00082 | 0.00006 | 0.08984 | 0.00149 | 0.49155 | 0.00356 |
| 0.18449 | 0.00127 | 0.02247 | 0.00065 | 0.00085 | 0.00008 | 0.10032 | 0.00116 | 0.00035 | 0.00004 |
| 0.18116 | 0.00145 | 0.01835 | 0.00083 | 0.00099 | 0.00007 | 0.13729 | 0.00113 | 0.00040 | 0.00003 |
| 0.19153 | 0.00174 | 0.01554 | 0.00071 | 0.00119 | 0.00008 | 0.16216 | 0.00139 | | |

Data Extracted from Bin (1993) Fig. 11

| X | Qa | X | Qa | X | Qa | X | Qa | X | Qa |
|---|---|---|---|---|---|---|---|---|---|
| 0.00019 | 0.00001 | 0.00297 | 0.00005 | 0.00486 | 0.00012 | 0.01480 | 0.00028 | 0.03663 | 0.00049 |
| 0.00024 | 0.00001 | 0.00224 | 0.00006 | 0.00468 | 0.00007 | 0.01370 | 0.00023 | 0.04279 | 0.00048 |
| 0.00027 | 0.00001 | 0.00202 | 0.00006 | 0.00506 | 0.00008 | 0.01251 | 0.00022 | 0.04686 | 0.00049 |
| 0.00030 | 0.00001 | 0.00173 | 0.00007 | 0.00547 | 0.00009 | 0.01235 | 0.00023 | 0.03569 | 0.00055 |
| 0.00037 | 0.00001 | 0.00164 | 0.00007 | 0.00568 | 0.00011 | 0.01157 | 0.00023 | 0.03757 | 0.00065 |
| 0.00037 | 0.00002 | 0.00175 | 0.00007 | 0.00553 | 0.00012 | 0.01099 | 0.00021 | 0.03521 | 0.00073 |
| 0.00037 | 0.00002 | 0.00184 | 0.00007 | 0.00560 | 0.00014 | 0.01173 | 0.00020 | 0.04622 | 0.00077 |
| 0.00049 | 0.00001 | 0.00204 | 0.00007 | 0.00461 | 0.00015 | 0.01085 | 0.00019 | 0.04564 | 0.00068 |
| 0.00048 | 0.00003 | 0.00209 | 0.00008 | 0.00480 | 0.00016 | 0.01057 | 0.00018 | 0.04010 | 0.00060 |
| 0.00054 | 0.00003 | 0.00238 | 0.00008 | 0.00539 | 0.00018 | 0.01085 | 0.00015 | 0.04390 | 0.00062 |
| 0.00053 | 0.00002 | 0.00235 | 0.00008 | 0.00560 | 0.00019 | 0.02021 | 0.00021 | 0.04506 | 0.00059 |
| 0.00057 | 0.00002 | 0.00229 | 0.00007 | 0.00567 | 0.00021 | 0.01600 | 0.00022 | 0.04745 | 0.00060 |
| 0.00060 | 0.00002 | 0.00279 | 0.00008 | 0.00605 | 0.00023 | 0.01539 | 0.00024 | 0.04998 | 0.00056 |
| 0.00060 | 0.00003 | 0.00294 | 0.00007 | 0.00663 | 0.00023 | 0.01600 | 0.00025 | 0.05196 | 0.00061 |
| 0.00069 | 0.00002 | 0.00305 | 0.00006 | 0.00698 | 0.00021 | 0.01752 | 0.00027 | 0.05331 | 0.00072 |
| 0.00073 | 0.00002 | 0.00422 | 0.00005 | 0.00698 | 0.00019 | 0.02183 | 0.00027 | 0.06308 | 0.00079 |
| 0.00079 | 0.00003 | 0.00356 | 0.00008 | 0.00613 | 0.00017 | 0.01917 | 0.00031 | 0.06998 | 0.00078 |
| 0.00065 | 0.00003 | 0.00321 | 0.00008 | 0.00663 | 0.00016 | 0.01729 | 0.00031 | 0.08285 | 0.00058 |
| 0.00065 | 0.00003 | 0.00313 | 0.00008 | 0.00606 | 0.00014 | 0.01917 | 0.00034 | 0.09303 | 0.00100 |
| 0.00069 | 0.00004 | 0.00301 | 0.00009 | 0.00630 | 0.00012 | 0.01821 | 0.00031 | 0.07464 | 0.00094 |
| 0.00081 | 0.00004 | 0.00264 | 0.00010 | 0.00699 | 0.00012 | 0.01751 | 0.00033 | | |
| 0.00098 | 0.00004 | 0.00271 | 0.00010 | 0.00717 | 0.00012 | 0.01558 | 0.00032 | | |
| 0.00111 | 0.00003 | 0.00290 | 0.00011 | 0.00745 | 0.00015 | 0.01558 | 0.00034 | | |
| 0.00122 | 0.00002 | 0.00293 | 0.00011 | 0.00717 | 0.00017 | 0.01620 | 0.00034 | | |
| 0.00089 | 0.00002 | 0.00286 | 0.00012 | 0.00775 | 0.00017 | 0.01558 | 0.00038 | | |
| 0.00135 | 0.00002 | 0.00317 | 0.00013 | 0.00816 | 0.00016 | 0.01404 | 0.00039 | | |
| 0.00187 | 0.00002 | 0.00347 | 0.00013 | 0.00871 | 0.00017 | 0.01351 | 0.00036 | | |
| 0.00140 | 0.00003 | 0.00356 | 0.00014 | 0.00816 | 0.00018 | 0.01993 | 0.00036 | | |
| 0.00120 | 0.00004 | 0.00411 | 0.00015 | 0.00905 | 0.00019 | 0.01892 | 0.00040 | | |
| 0.00095 | 0.00005 | 0.00444 | 0.00015 | 0.00882 | 0.00021 | 0.01773 | 0.00044 | | |
| 0.00101 | 0.00006 | 0.00438 | 0.00014 | 0.00784 | 0.00023 | 0.01941 | 0.00047 | | |
| 0.00130 | 0.00005 | 0.00421 | 0.00013 | 0.00795 | 0.00026 | 0.02126 | 0.00047 | | |
| 0.00140 | 0.00004 | 0.00356 | 0.00012 | 0.00837 | 0.00029 | 0.02126 | 0.00041 | | |
| 0.00164 | 0.00004 | 0.00366 | 0.00011 | 0.00905 | 0.00024 | 0.02421 | 0.00033 | | |
| 0.00184 | 0.00004 | 0.00338 | 0.00010 | 0.00953 | 0.00025 | 0.02685 | 0.00033 | | |
| 0.00184 | 0.00005 | 0.00334 | 0.00009 | 0.00952 | 0.00028 | 0.02828 | 0.00039 | | |
| 0.00173 | 0.00005 | 0.00356 | 0.00009 | 0.00940 | 0.00034 | 0.02420 | 0.00040 | | |
| 0.00144 | 0.00005 | 0.00380 | 0.00008 | 0.01172 | 0.00031 | 0.02452 | 0.00043 | | |
| 0.00150 | 0.00005 | 0.00400 | 0.00008 | 0.01098 | 0.00029 | 0.02482 | 0.00057 | | |
| 0.00164 | 0.00005 | 0.00427 | 0.00009 | 0.01142 | 0.00027 | 0.02754 | 0.00049 | | |
| 0.00168 | 0.00005 | 0.00416 | 0.00010 | 0.01203 | 0.00029 | 0.02863 | 0.00053 | | |
| 0.00150 | 0.00006 | 0.00395 | 0.00010 | 0.01267 | 0.00030 | 0.03054 | 0.00059 | | |
| 0.00179 | 0.00006 | 0.00462 | 0.00009 | 0.01219 | 0.00026 | 0.03176 | 0.00052 | | |
| 0.00207 | 0.00005 | 0.00400 | 0.00011 | 0.01300 | 0.00027 | 0.03095 | 0.00049 | | |
| 0.00218 | 0.00005 | 0.00438 | 0.00010 | 0.01334 | 0.00029 | 0.03303 | 0.00046 | | |
| 0.00227 | 0.00005 | 0.00462 | 0.00010 | 0.01369 | 0.00026 | 0.03712 | 0.00042 | | |
| 0.00272 | 0.00004 | 0.00480 | 0.00011 | 0.01387 | 0.00027 | 0.03389 | 0.00049 | | |
| 0.00251 | 0.00005 | 0.00450 | 0.00011 | 0.01442 | 0.00025 | 0.03808 | 0.00051 | | |

Current Data

| X | Qa | X | Qa |
|---|---|---|---|
| 0.00677 | 0.00247 | 3.58681 | 0.01538 |
| 0.01971 | 0.00203 | 3.58681 | 0.01796 |
| 0.03776 | 0.00014 | 4.42623 | 0.01773 |
| 0.06049 | 0.00073 | 5.34387 | 0.02048 |
| 0.06049 | 0.00245 | 5.34387 | 0.02041 |
| 0.08767 | 0.00138 | 6.33959 | 0.02248 |
| 0.11913 | 0.00174 | 7.41381 | 0.02677 |
| 0.15474 | 0.00229 | 7.41381 | 0.03009 |
| 0.19439 | 0.00302 | 8.56267 | 0.03016 |
| 0.23799 | 0.00366 | 9.78670 | 0.02819 |
| 0.28547 | 0.00452 | 9.78670 | 0.02496 |
| 0.28547 | 0.00552 | 0.12195 | 0.02165 |
| 0.33677 | 0.00537 | 0.58568 | 0.02238 |
| 0.39183 | 0.00632 | 1.99351 | 0.01901 |
| 0.45059 | 0.00696 | 4.12694 | 0.02270 |
| 0.51302 | 0.00758 | 6.94294 | 0.02387 |
| 0.51302 | 0.00911 | | |
| 0.07551 | 0.00626 | | |
| 0.24350 | 0.00700 | | |
| 0.24350 | 0.00776 | | |
| 0.49166 | 0.00694 | | |
| 0.81482 | 0.00951 | | |
| 0.81482 | 0.01044 | | |
| 1.20971 | 0.01728 | | |
| 1.67394 | 0.03081 | | |
| 1.67394 | 0.03094 | | |
| 2.20566 | 0.04016 | | |
| 2.80337 | 0.03963 | | |
| 2.80337 | 0.03937 | | |
| 3.46579 | 0.03931 | | |
| 4.19183 | 0.03546 | | |
| 4.19183 | 0.03427 | | |
| 4.98054 | 0.03773 | | |
| 5.83107 | 0.03817 | | |
| 5.83107 | 0.03604 | | |
| 6.74266 | 0.03841 | | |
| 7.71461 | 0.04098 | | |
| 7.71461 | 0.03811 | | |
| 0.10247 | 0.00634 | | |
| 0.32268 | 0.00741 | | |
| 0.32268 | 0.00994 | | |
| 0.64335 | 0.00851 | | |
| 1.05795 | 0.01063 | | |
| 1.05795 | 0.01028 | | |
| 1.56298 | 0.01143 | | |
| 2.15400 | 0.01179 | | |
| 2.15400 | 0.01313 | | |
| 2.82925 | 0.01335 | | |